Adenosine-induced elimination of redox intercalators from dsDNA-aptamer conformational switches

by

YunDai

B.Sc., Simon Fraser University, 2010

Thesis Submitted in Partial Fulfillment
of the Requirements for the Degree of
Master ofScience

in the
Department of Chemistry
Faculty of Science

Approval

Name: **YunDai**

Degree: **Master ofScience**

Title of Thesis: ***Adenosine induced elimination of redox intercalators from dsDNA-aptamer conformational switches***

Examining Committee:

Chair: **Dr. Tim Storr**, Assistant Professor

Dr. Hua-Zhong Yu
Senior Supervisor
Professor

Dr. Dan Bizzotto
Supervisor
AssociateProfessor

Dr. Bing-YunSun
Supervisor
AssistantProfessor

Dr.Hsien-Chang Chang
Examiner
Professor
Department of Biomedical Engineering, National Cheng Kung University

Date Defended/Approved: July12, 2012

Partial Copyright Licence

Ethics Statement

The author, whose name appears on the title page of this work, has obtained, for the research described in this work, either:

a. human research ethics approval from the Simon Fraser University Office of Research Ethics,

or

b. advance approval of the animal care protocol from the University Animal Care Committee of Simon Fraser University;

or has conducted the research

c. as a co-investigator, collaborator or research assistant in a research project approved in advance,

or

d. as a member of a course approved in advance for minimal risk human research, by the Office of Research Ethics.

A copy of the approval letter has been filed at the Theses Office of the University Library at the time of submission of this thesis or project.

The original application for approval and letter of approval are filed with the relevant offices. Inquiries may be directed to those authorities.

Simon Fraser University Library
Burnaby, British Columbia, Canada

update Spring 2010

Abstract

Immobilization and electrochemical characterization of specially designed DNA-aptamer constructs (namely, “DNA conformational switches”) are of great importance for the development of versatile biosensorsand the fundamental understanding of DNA-ligand interactions. Wehave created andimmobilizedadsDNA-anti-adenosine aptamer construct on gold which is expected to undergo structural changes upon binding adenosine.In particular,methylene blue (MB), a solution-diffused redox marker, was used as a model system to probe the rather complex interaction modes between small redox molecules and surface-bound DNA switches. Besides intercalating with the double-stranded DNA stem, MB can stack with a single guaninebase in the relatively unstructured aptamer domain or electrostaticallybindtothe DNA backbone. The decreased surface density of MB after adenosine binding indicated that the ligand-gated structural change of the dsDNA-aptamer construct can eliminate MB molecules that were originally bound to the aptamer domain, but not those in the complementary stem.

Keywords: DNA-aptamer; electrochemistry; self-assembled monolayers, biosensor; methylene blue

To everyone who guided me and helped me

Acknowledgements

I would like to expressmy sincere gratefulness to my senior supervisor, Dr. Hua-Zhong (Hogan) Yu, for his patient and supportive guidance since I joined his team. I give my sincere thanks to my committee members, Dr. MelanieAlexis O'Neill, Dr. Bingyun Sun and Dr. Dan Bizzotto, for their friendly, open and creative advice. I would like to thank our guests, Dr. Chii-WannLin from National Taiwan University and Dr. Hsien-ChangChang from National Cheng Kung University, for sharing their time tobe my examiners of this thesis. I would like to thank Dr. Michael Eikerling and Dr. DipankarSen for teaching me fundamental concepts of electrochemistry and nuclei acids in classes.I also give my special thanks to Dr. BananiChakraborty and Dr. BixiaGe for helping me start my work and to all my lab mates for everyday discussion and encouragement. I appreciate Dr.EberhardKiehlmann for editing the thesis and helpful suggestions.Furthermore, I thank everyone in the Faculty of Science. Everyone here loves science and inspires with passion. Not only scientific knowledge I learned here in the past two years, I also learned critical, analytical and creative thinking, and more importantly how to be a supportive team player.

Table of Contents

List of Tables

List of Figures

List of Acronyms andGlossary

A/T/C/G	adenosine/ cytidine/ thymidine/ guanosine
A/C/T/GMP	adenosine/ cytidine/ thymidine/ guanosine 5’-monophosphate
A/C/T/GTP	adenosine/ cytidine/ thymidine/ guanosine 5’-triphosphate
dA/dT/dC/dG	deoxyadenosine/ deoxythymidine/deoxycytidine/ / deoxyguanosine
AQ	Anthraquinone
apt-DNA	the dsDNA aptamer construct
comp-DNA	the complementary DNA duplex
b.p.	base pair
CV	cyclic voltammogram
DNA	deoxyribonucleic acids
dsDNA	double strand deoxyribonucleic acid
ssDNA	single strand deoxyribonucleic acid
EA	electron acceptor
ED	electron donor
EEC	electron-electron-chemical mechanism
ECE	electron-chemical-electron mechanism
CEE	chemical-electron-electron mechanism
EPR	electron paramagnetic resonance
E_{pa}	anodic peak potential
E_{pc}	cathodic peak potential
E^o	standard potential
$E^{o'}$	formal potential
ΔE/delta E	E_{pa} - E_{pc}
Fcc	face-centered cubic
FRET	fluorescence resonance energy transfer
FTIR	fourier transform infra-red spectroscopy
ΔG	Gibbs free energy difference
i_p	peak current
i_{pa}	anodic peak current
i_{pc}	cathodic peak current
K	equilibrium constant
K_d	dissociation constant

$\boldsymbol{\kappa}$	heterogeneous electron transfer rate constant
$\mathscr{k}$	homogeneous electron transfer rate constant
LB	leucomethylene blue
MB	methylene blue
MCH	6-mercapto-1-hexanol
MCU	11-Mercapto-1-undecanol
MUA	11-mercapto-1-undecanoic acid
NMR	nuclear magnetic resonance
NHE	normal hydrogen electrode
NOEs	nuclear Overhauser effects
PCR	polymerase chain reaction
RH	relative humidity
RNA	ribonucleic acids
SAMs	self-assembled monolayers
SCE	saturated calomel electrode
SELEX	systematic evolution of ligands by exponential enrichment
STM	scanning tunneling microscope
XPS	X-ray photoelectron spectroscopy

1. General Introduction

The 20th century was the knowledge explosion era; in many fields, numerous science and technology discoverieswere made with a tremendous speed. During this period of time, multi-disciplinaryinteractions becamemore and more frequent; many inter-disciplines such as bio-physics, bio-informatics and biochemistry have emerged. DNA-based electrochemical biosensorswereone of the outcomes of interdisciplinary research.It combines two concepts: functional deoxyribonucleic acids (DNA) and electrochemistry. Our group has been working on the development of electrochemical biosensors during the last decade, and a part of my work is about “label-free” electrochemical biosensors using solution-diffused methylene blue as redox marker. To understand the previous work of our group and the present project, a brief introduction to thesurface chemistry of DNA and functional DNA constructs is givenbelow.

1.1. DNA and its chemical property

In 1868, Swedish scientist Friedrich Miescher first precipitated‘nuclein’from pure cell nuclei of pig stomachs. More pure nuclein was crystallized by him from the sperm of Rhine salmon; the pure nuclein was acidic and existed in a salt form with a nitrogenous base. Nuclein, in fact, is a nucleo-protein and Richar Altman coined the term ‘nucleic acid’ in 1898 when he obtained the first protein-free material from nuclein.Prior to the breakthrough findings of Watson and Crick, Klein and Thannhauserobtained the four

crystalline deoxyribonucleotides in 1935.[1]Thestructures of the mononucleotides are shown in Figure 1-1.

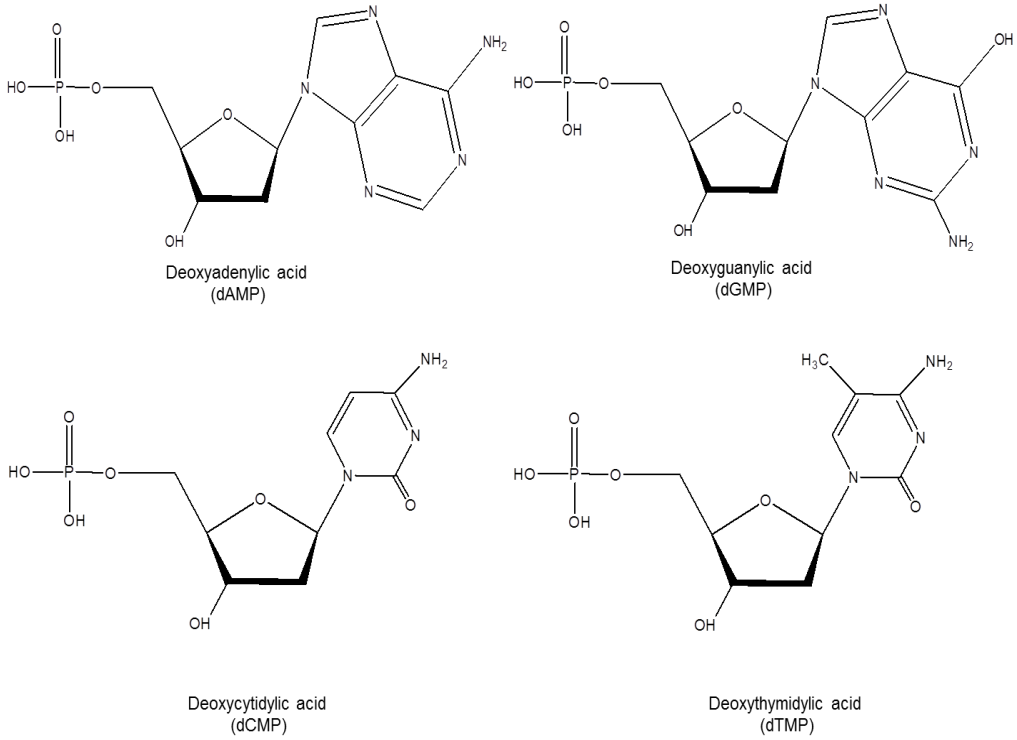

Figure 1-1. Structure ofdeoxyribonucleotides.

Two decades later, Watson and Crick's discovery revealed the anti-parallel double helical structure ofduplex DNA which mainly consists of Watson-Crick base-pairsheld together via hydrogen bonding and base stacking. Then, it was found that the secondary structure of duplex DNA could be categorized into three main conformation types including A-DNA, B-DNA and Z-DNA.In the early phases of investigation of the secondary structure, X-ray diffraction studies have shown that at low humidity, most synthetic oligonucleotides are of the A-DNA type, and B-DNA is mainly found at high relative humidity (95% RH). Although A-DNA and B-DNA duplex are different in average rise per-pair, helix rotation per pair and sugar pucker, they both have right-handed

helical structures, anti-glycosidicbonds and one phosphate peak in NMR spectra. However, Z-DNA duplex which forms in unusual conditions such as organic solvent (ethanol), high salt concentration (~2.5 M NaCl),and specific oligomer sequenceshas two phosphate peaks in NMR spectra and alternating *syn*-and *anti*-glycosidicbonds. Unlike the A-DNA and B-DNA duplexes which only have $C^{3'}$-*endo* and $C^{2'}$-*endo* sugar pucker respectively, the Z-DNA duplex has alternating $C^{2'}$-*endo* for the *anti*-residues and $C^{3'}$-*endo* for the *syn*-residues. Generally speaking, at physiological conditionsthe B-type DNA structure is the predominate form.[2]

1.1.1. Reversible interaction of DNA with small molecules

DNA duplex can interact reversibly with a broad range of chemical species in three primary ways including (a) electrostatic interaction, (b) groove-binding and (c) intercalation.Figure 1-2 illustrates these three binding modes with a B-DNA duplex.

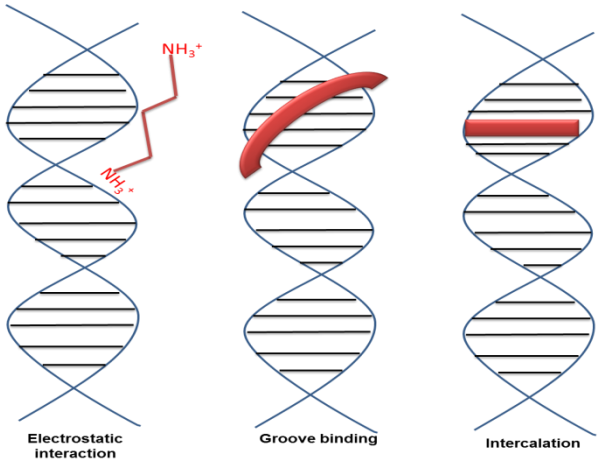

Figure 1-2. Binding modes for small molecules with a B-DNA duplex.

Due to anionic phosphate groups, DNA is highly negatively charged. If a B-DNA oligomer is modelled as an ideal linear rod, then there is one negative charge per 1.7 Å(approximately two charges per base pair).Manning and coworkers have shown

thatone molecule in solution would not be stable until the line charge density is smaller than one charge per 7 Å(as one Bjerrum length is approximately equal to 7 Å in water). Thus counter ions (such as Na^+, Li^+, Mg^{2+}) from solution must help DNA oligomers to achieve a stable conformation; this phenomenon is called counter ion condensation. With the B-DNA duplex, this condensation results in an average of 0.88 counter ions per phosphate group. Besides counter ions,at low salt concentration (~0.1 M)planar aromatic cations(such as proflavine)can also interact with DNA through non-specific outside stacking and lead to a release of condensed counter ions.[3-5]

Small molecules (such as distamycin, Hoechst 33258) are also mainly minor-groove binding molecules. Typically, they have a crescent shape consisting of several simple aromatic rings which are linked with torsional freedom to allow a twist to fit into the DNA minor groove and have NH groups on the interior of the crescent to form hydrogen bonds with A:T base pairs. In addition, electrostatic interactions between cation groups and negative electrostatic potential in the minor groove plus van der Waals force from the close contact with the walls of the minor groove enforce the groove binding.[5]

In the 1960s, concluding from previous studies that planar aromatic molecules could bind to DNA duplexes, Lerman coined the term intercalation.[6]The creation of the intercalation sites can cause an untwisting of the double helix, a separation of base-pairs and a lengthening of the double helix, but these changes vary with different intercalators. For example, daunomycin would create a 3.4 Å base separation and 8º unwound helical twist angle, while methylene blue may cause a 7.2Å base separation and 19º unwound helical twist angle.[5]Theoretically, there are ten possible dinucleotide combinations to

form potential intercalation sites for simple intercalators (intercalators having only one binding site) (Figure 1-3).

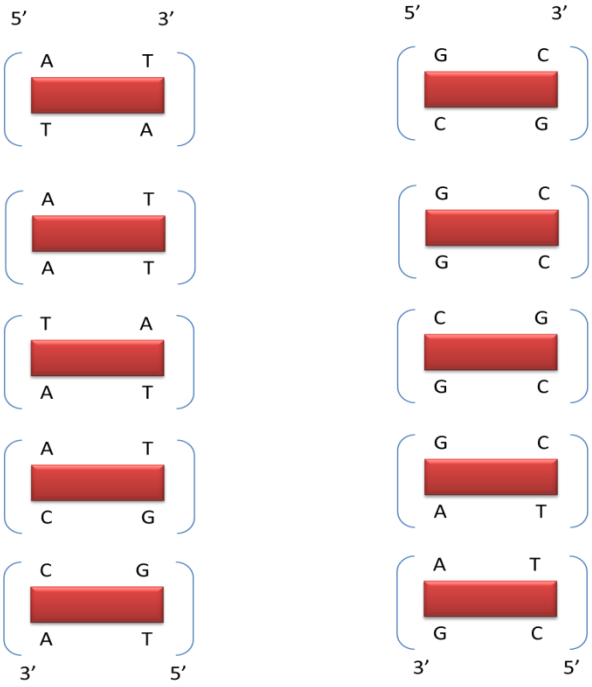

Figure 1-3. The ten possible dinucleotide combinations to form intercalation sites

Most simple intercalators either have no binding site preference or a slight G:C sites preference. It has been suggested that the larger intrinsic dipole moment of G:C base pairs and the ability of G:C base pairs to induce polarization in the ring system of intercalators can lead to the G:C sites preference. In theory, a DNA duplex can be constructed with intercalators at all possible intercalation sites, however, empirical observations show that a simple intercalator can reach saturation at a maximum of one intercalator per two base pairs in solution; this is called the neighbour exclusion principle.[5,]

Intercalators share structural similarities with minor groove binding molecules. For example they both usually have aromatic rings. But they can be differentiated by fluorescence resonance energy transfer (FRET) and viscosity measurement. In a FRET measurement, the DNA is excited and the energy can only be transferred from the excited DNA to intercalators but not to groove binding molecules because intercalators are closer to base pairs than groove binding molecules. Viscosity measurement also was used to differentiate groove binding molecules and intercalators, because intercalators cause a lengthening of the double helix while groove binding molecules do not change the length of the double helix and viscosity measurement is sensitive to such a length change. However, except FRET and viscosity measurement, simple fluorescenceand florescence quenching experiments donot show a clear difference between groove binding molecules and intercalators. For instance, both groove binding molecules and intercalators will have a red shift in their excitation wavelength and an increment in fluorescence intensities when they bind to a DNA duplex. In addition,both groove binding molecules and intercalators can be saved from fluorescence quenching because the negatively charged phosphate backbone of DNA repels the quencher (iodide).[5,7]

1.1.2. DNA-mediated charge transfer

Charge transfer through DNA was first proposed by Eley and Spovey 50 years ago.[8]Inthe 1990s, scientists found relative appropriatetechnologies to test and verify this assumption. Earlier, controversial results were obtained showing that DNA is a superconductor,semiconductor, conductoror insulator.[9-12]This controversy triggered intense research, and later more experimental results indicated that DNA could conduct charge. Generally speaking, tworeasonablemechanisms have been proposed: a)

thehole-hopping mechanism and b) the electron-tunnelling mechanism. The hole-hopping mechanism is responsible for a long-range charge transfer through DNA;[13] the electron tunnellingmechanism could explain short-range charge transfer through DNA.[14]Hole-hopping process can be initiated photochemically by excitation of a photosensitizer (suchas Ru(III) complex) that is covalently attached and end-stackedto/with a DNA duplex. Then anelectron hole(positive charge) would be generated on the proximal guanine and transfer to the next guanine immediately. A GGG (or GG) sequence would have a stronger affinity to the electron hole than single G, thus a GGG (or GG) sequence usually would be utilized as an electron-hole accepting group in DNA oligomerdesign. But the electron hole could also be captured by water molecules in the solvent and accordingly the charge transfer process through DNA would eventually cease. Unlike the hole-hopping process, the electron tunnelling process is strongly distance-dependent. Base pairs could be considered as a bridgeseparating the electron donor (ED) and electron acceptor (EA) and the electron transfer rate constant could be expressed in a simple equation:

$$\hbar_{et} = \hbar_o e^{-\beta R}$$ (Equation 1-1)

whereR is the ED-EA center-to-center distance and$\boldsymbol{\beta}$ is dependent uponthe nature of the bridge and its coupling with ED and EA.[15]

Fluorescence spectroscopy is one of the major methods to study DNA conductivity.Bartonand co-workers first employed DNA intercalators includingpolypyridyl complexesof Ru(II) as “electron hole” acceptor and Co(III) complexes as “electron hole” donor to study the DNA conductivity by fluorescence spectroscopy.[16] In order to precisely define the position of an electron donor and acceptor in aDNA duplex, Kelley

covalently attached ethidium and Rh(III) complex to opposite ends of the duplex (Figure 1-4).[17]

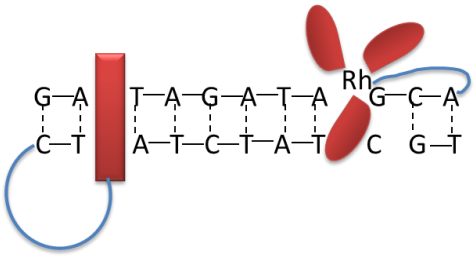

Figure 1-4. Ethidium and Rh(III) complexestethered to dsDNA for charge transfer studies.

Oneethidium duplex oligomer, made by hybridization of an ethidium-modified15-mer strand to an unmodified complement, showed significant luminescence. In contrast, in another 15-mer oligonucleotide duplex,containing the ruthenium intercalator tethered to the 5'-end of one strand andethidiumtethered to the 5'-end of the other strand, no luminescence was evident. This is because that Rh(III) complex eventuallycaptured the energy transferred from excited ethidiumthroughthe DNA oligomer. In addition to the transitionmetal complex, guanine itself in a DNA duplex was also used as electron donor in aspectroscopy study.[18]

Gel shift assayvia DNA oxidation lesion is another common method applied in DNA conductivity studies. The terminal G at the 5'-end of 5'-GGG-3' or 5'-GG-3' sequences is usually acting as an electrondonor. The other end of the DNA would be labelled with a photo-sensitizer to initiate the hole-hopping mechanism under irradiation. The advantage of this method is that after treatment with piperidine, we can observe the final result, charge-transfer-inducedDNA cleavageby running gel electrophoresis assay.[19]

Electrochemical methods to study DNA conductivity have been developed in the last two decades.For an example, one end (usually the 3'-end) of an oligonucleotide could be covalently modified with a redox marker(e.g.,ferrocene or methylene blue); and theother end (usually the 5'-end) of its complementary oligonucleotide with a thiol group. After hybridization, the thiol-modified end can be immobilized on the surface of a gold electrode to form a self-assembled monolayer (SAM) of the DNA duplex. We can detectthe electrochemicalsignal generated by the redox marker by applying a voltage to the SAM-modified gold electrode. The advantage of this electrochemical method is that we can conduct an experimentquickly and study the kinetics of the electron transfer through DNA.

1.1.3. Surface chemistry of DNA on Au(111) surface

Self-assembled monolayers (SAMs) of DNA on solid surfaces have obtained intense research attention becausethey are basic platforms for developing DNA-chips.[20] The Au (111) surface is commonly used for preparing DNA SAMs, and both its electrochemicalproperties and surface structure have been studied. Using 0.1M $HClO_4$ as electrolyte,the Au (111) surface would undergo a redox process between 1and 1.5 V (vs. NHE). The Au atoms on the surface can be oxidized first (two anodic peaks are observed at 1.3 and 1.5 V (vs. NHE)); then the formed Au oxides can be reduced back to Au and a sharp peak is observed at 1 V (vs.NHE).[20]This redox process is described as below:

$$Au + nH_2O \longrightarrow Au(OH)_n + nH^+ + ne^- \qquad \text{(Equation 1-2)}$$

$$Au(OH)_n + ne^- \longrightarrow Au + nOH^- \qquad \text{(Equation 1-3)}$$

Usually in acid solution (e.g. 0.5 M H_2SO_4), no redox peak isobserved below 0.88 V and the background currentinthis regionisneither from the redox of Au (111) nor from the redox of solvent, but mainly contributed by capacitive current of the double layer at the electrode-solution interface. This low-background current allowsthe Au (111) electrode to maintain a high signal to noise ratio, which is helpful in sensing weak signals.The surface structure of Au (111) has been investigated by scanning tunnelling microscopy (STM).[20]It was reported that the distance between two close Au atoms is 2.89 Å. The angles between the atomsare 60º or multiples of 60º, indicating a face-centered cubic (fcc) lattice structure.

Like many other alkanethiolateSAMs, DNA SAMs on aAu (111) surface are formed via chemisorption through gold-sulphur bonds. This chemisorption requires activation of the S-H bonds of the alkylthiolwhich is covalently bound to the terminalphosphate moiety of DNAthrough C-O bonds. However, the fate of the hydrogenatoms of the S-H groups of the alkylthiol is not clear and controversial.[21]It seemsthat adsorption of alkylthiolsin vacuum leads to reduction of this hydrogen and results in the production of H_2; in a non-vacuum condition, oxygen existing in solution may oxidize this hydrogen to water.[21] Nevertheless, the mystery of the hydrogen is not an obstacle to studySAMs on Au surfaces.Several studies have estimated that the strength of the gold-sulphur bond is in therange of 120 - 200 kJ/mol, which is in the order of covalent bond strengths.[21]Hence, the Au-S bondis sufficient to retain the DNA SAMs on the Au surface in a durable fashion. DNA SAMs on Au surfaces have been investigated by various techniques.Tarlov et al. have characterized DNA SAMs immobilized on a Au surface systematicallyby using STM, X-ray photoelectron spectroscopy (XPS), and Fourier transform infra-red spectroscopy (FTIR).[22-25]They

concluded that a) DNA can non-specifically adsorb on a Au surface without a S-Au bond; b) thiol-modified long oligonucleotides (b.p. >24) have a more disordered structure and lower surface density than short oligonucleotides; c) co-immobilization of 6-mercaptol-1-hexanol (MCH) (later called “spacer”) with DNA can remove non-specifically adsorbed DNA and result in a more ordered DNA SAM. A two-step protocol to form DNA SAMs proposed by Tarlov et al. has been widely accepted in the community, in which the Au surface is first exposed to a micromolarsolution of thiol-modified DNA and then to a millimolar solution of MCH. Surface densities of ssDNA and dsDNA SAMsas high as3 x 10^{13} and 5 x 10^{12} molecules/cm^2,respectively,[25]could beideally achieved.Recently,wehave investigated the non-uniformity of the DNA-modified gold electrodes via electrochemical in situ fluorescence microscopy, and found that the modification of gold surface withwiththiol-tethered single -stranded DNA followed by MCH passivation in fact resultsin a heterogeneous rather than a homogeneous packing density.[81]

1.2. **DNA aptamers**

The term “aptamer” is derived from the Latin word “aptus”, meaning “to fit”. Aptamers are functional biochemical molecules (e.g.,nucleic acids, peptides) that have a specific binding affinity to a certain target. Ribonucleic acids (RNA) aptamers were first *in vitro* selected in1990 and the first DNA aptamer was reported in 1992.[26-28]Duringthe last two decades, aptamers for various targets (e.g. proteins, metal ions, and drugs) have been identified. The potential application ofaptamers in diagnostics attracted intensive interest; compared with traditional biosensors using antibodies as probes, biosensors using aptamers as probes (aptamer-based biosensors) generally are

believed to have three advantages. Firstly, aptamer-based biosensors have a broader range of targets including heavy metals, small molecules, even cells.Secondly, after being selected, aptamers (nucleic acids or peptides) can be easily synthesized in a commercial manner and DNA aptamers are generally more chemically stable than antibodies or enzymes.Thirdly, aptamers usually would undergo conformational change upon target binding and this conformational change allows us to design diverse aptamer-based biosensors. Besides the application in diagnostics, DNA aptamers also show promising therapeuticalapplications. For example, anti-thrombin DNA aptamers with a high affinity (K_d= 25 nM) may be used as anti-coagulants.[29]

1.2.1. In vitro selection of DNA aptamers

Natural selection is the basic process of biological evolution; *in vitro* selection (systematic evolution of ligands by exponential enrichment, SELEX) of nucleic acids developed in 1990s mimicked the process of natural selection and began a new age in the application of functional nucleic acids.[26-28]

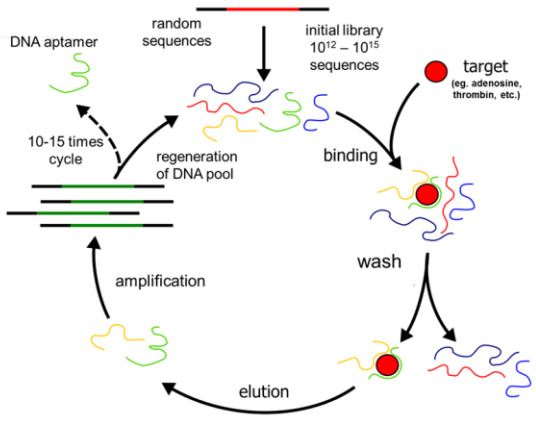

Figure 1-5. The in vitro selection process of a DNA aptamer

The basic principle of *in vitro* selection is using affinity chromatography to select aptamers from a library of oligonucleotides, which typically contains 10^{12} - $10^{15}$of random10-100 nucleotides long oligonucleotides. Single-strand nucleic acids are required here, as the nucleic acids within this library need to be free to fold into a wide range of tertiary structures. For DNA aptamers, once the library of oligonucleotides is set, we can apply affinity chromatography, in which targets are immobilized on a solid support, to select potential aptamers and those potential sequencescan be directly amplified by PCR. Then, after repeating several cycles of affinity chromatography and PCR, we can determine the candidate sequences with relatively high affinity for specific targets (Figure 1-5).In order to improve the specificity of aptamers, counter-affinity chromatography may be used as an assist.

1.2.2. Anti-adenosine DNA aptamer and its application

An adenosine moiety is present in many biological cofactors.For example, adenosine triphosphate (ATP) plays an important role in many biological reactions. In 1993,Szostak et al. isolated one RNA aptamer which binds to both adenosine and ATP and theyexplored the potential ability of an RNA aptamer to catalyze reactions involving ATP or adenosine.[30]Subsequently, Szostak et al. isolated DNA aptamers for ATP / adenosinein 1995; the reported DNA aptamer can bind to both ATP and adenosine with a similar dissociation constant (K_d =3-9 M).[31]Two years later, a nuclear magnetic resonance (NMR) study investigated the tertiary structure of this anti-adenosine DNA aptamer and its adenosine monophosphate (AMP)-DNA aptamer complex.[32]Patel et al. reported that two equivalent AMP molecules would cooperatively bind to this DNA aptamer; mutation experiments showed that two guanine substitutions by inosine led to no AMP binding which indicates that AMP molecules bind to G9 and G22. In addition,2-

dimensional NMR identified sixbase pair mismatches (G18·A10, G5·A23, G8·G19, G21·G6, AMP_I·G9 and AMP_{II}·G22). The G18·A10and G5·A23 mismatchesare defined by strongnuclearOverhauser effects**(**NOEs**)**between the amino proton of G18 or G5 and the proton of A10 or A23, respectively. (NOEs are observed when two hydrogen atoms are in close proximity to each other, resulting in a transfer of nuclear spin polarization from one nuclear spin population to another via cross-relaxation.)The G8·G19and G21·G6mismatchesaredefined by strong NOEs between the imino proton of G8 or G21and theproton of G19 or G6, respectively. An AMP_I·G9 or AMP_{II}·G22recognition mismatch is defined by strong NOEs between the amino proton of G9 or G22and theproton of AMP_I or AMP_{II}.According to molecular dynamics calculations,two AMP molecules bind in an expanded rectangular minor groove binding pocket as described below: The G18·A10 (G5·A23) mismatch is of the sheared G·A type which involves the pairing of the minor groove of guanine withthe Hoogsteen edge of adenine. TheG8·G19 (G21·G6) mismatch is of the reversed Hoogsteen G·G type which involves the pairing of the Watson-Crick edge of G8 (G21) and the Hoogsteen edge of G19 (G6). TheAMP_I·G9 (AMP_{II}·G22) recognition mismatch involves the pairing of the minor groove of guanine withthe Watson-Crick edge of adenine; G8, G19 and A20 are in the same plane forming a triple-base platform; G21, G6 and G7 form another triple-base platform. Besides hydrogen bondingof non-conventional base pairs and obvious base stacking of triple-base platforms, thereis also intensive cross-strand stacking to support the AMP-DNA aptamer complex. Such cross-strand stacking can be found between G7 and G8, A20 and G21, G6 and G19, and G9 and G18. Thestereo view of this AMP-DNA aptamer complex is shown in Figure 1-6.

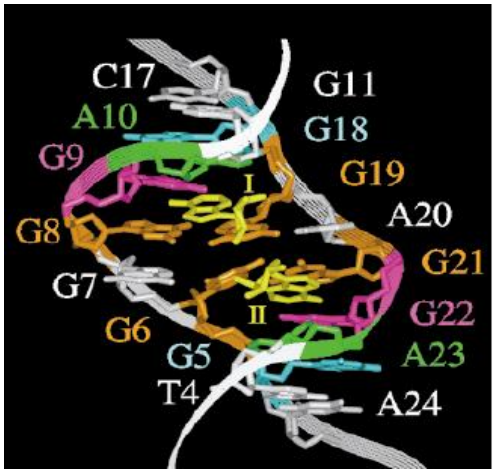

Figure 1-6. The stereo view of the AMP-DNA aptamer complex

Note: Lin (1997); used with permission.

Although the structure of the AMP-DNA aptamer complex has been studied by Patel et al., details about the folding process of this aptamer are ambiguous. Nevertheless, Patel suggested that aptamers frequently show induced-fit folding behaviour.[33]Unstructured aptamers in solution undergo compaction to form stable structures upon binding targets. In 2001, Sen et al. utilized this induced-fit folding property of aptamers to construct an "integrated ligand sensor" (Figure 1-7).[34]

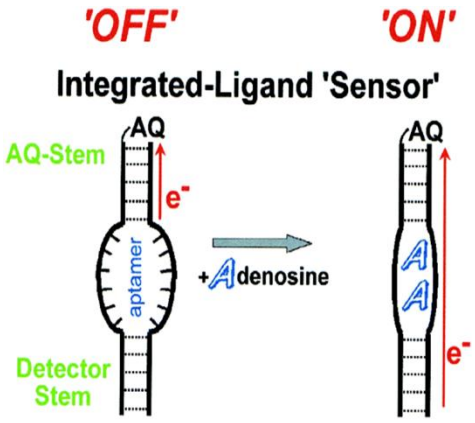

Figure 1-7. The "IntegratedLigand Sensor". AQ: anthraquinone.

Notes: Sen (2002); used with permission.

An aptamer domain was integrated into a piece of carefully designed double strand DNA which was thereby divided into an “upper”part (AQ-stem) and a “bottom” part (detector stem). Covalently attached anthraquinone (AQ) at the terminus of one strand can be photo-excited to act as an oxidant to withdraw electrons from the GG doublets, which locate at the AQ-stem and at the detector stem separately. After a piperidine treatment, the ratio between damaged GG doublets in thedetector stem and GG doublets in the AQ-stem (the cleavage ratio) can be quantifiedusing the phosphorimager trace of a sequencing gel electrophoresis.Sen et al. stated that the cleavage ratio increased after an incubation of ATP with suchan “integrated-ligand sensor”; charge transfer was confined within the AQ-stem, but extended to the detectorstem upon ATP-binding, and a linear detection range was found between 10 M to 500 M.[34]

1.3. **DNA-aptamer-based electrochemical biosensors**

Biosensors are analytical devices made of biological recognition elements and typically for the detection of biomedically relevant analytes through optical and electrochemical readout. They consist of three basic components: a) a biological sensing platform to recognize analytes, b) a transducing element to convert a biological recognition (conformational change) to a readable optical or electrochemical signaland c) a digital data processing device for end users. So far, various biological molecules (e.g., antibodies, peptides, aptamers,etc.) have been employed as recognition platforms. Antibody-based biosensors may be more widely adopted; meanwhile, the development of aptamer-based biosensorshas been growing fast and signal transduction via electrochemistry is a major method developed and used in our group.

Typically, conformational changes of an aptamer upon binding targets do not generate any feasiblesignal; thus a transducing method is required to express such conformational changes.[20,35]Plaxco and coworkers developed anaptamer-based electrochemical biosensor to detect thrombin (as illustrated in Figure 1-8 (a)).[35] Anti-thrombin DNA aptamers(single stranded DNA) covalently modifiedat both ends with methylene blue (MB) and thiol are immobilized on a gold electrode. Plaxco and coworkers observed a decreased peak current after adding thrombin. Theyproposed that anti-thrombin DNA aptamer on the electrode is likely unfolded and this conformational change allows electron tunnelling from tethered MB to the electrode.Upon thrombin binding anti-thrombinthe DNA aptamerwould form a G-quadruplex andthe distance between the tethered methylene blue and the electrode surface will increase, resulting in diminished electron tunnelling. Our group also applied covalentlytethered redox markers (e.g. ferrocene) to develop aptamer-based biosensors to detect thrombin. Instead of single strand DNA, we immobilized a rationally designeddouble-helical DNA/anti-thrombin aptamer construct on gold electrodes (as illustrated in Figure 1-8(b)).[36]Upon thrombin binding, an increased peak current was observed.Considering supportive results from the biochemical method via DNA oxidation lesion, we believe that thrombin binding-induced realignment of the double helical stems would facilitate the DNA-mediated charge transfer between Fc and the gold electrode.

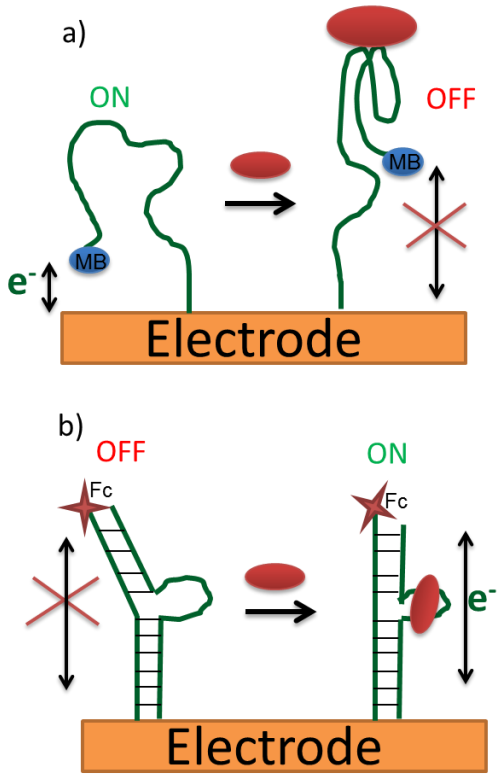

Figure 1-8. Aptamer-based biosensors with covalentlytethered redox makers.

Note: modified from Refs. 35 and. 36 with permission.

1.3.1. Aptamer-based electrochemical biosensors with solution-diffusedredox markers

Due to the relative synthetic complexity of covalent modification of DNA, researchers have also tested the solution-diffusedredox markers in the design of aptamer-based electrochemical biosensors. As we discussed, various types of molecular interactions are involved when small molecules bind to DNA, such as electrostatic, hydrogen bonding, and base stacking interactions. Our group hasrecently developed a "label-free" aptamer-based biosensor for lysozyme based on the electrostatic interaction between a redox metal complex, $[Ru(NH_3)_6]^{3+}$,and an anti-lysozyme DNA aptamer (as illustrated in Figure 1-9).[37]Whenanti-lysozyme DNA aptamers (single-stranded DNA)are

immobilized on gold electrodes, solution-diffused $[Ru(NH_3)_6]^{3+}$replaces the native counter ions (e.g., Na^+) associated withthe phosphate backbone, resulting in a pair of surface redox peaks for $[Ru(NH_3)_6]^{3+}$in the cyclic voltammogram. After incubation with lysozyme, we observed a decreased peak current for the surface-bound$[Ru(NH_3)_6]^{3+}$. It is evident that once positively charged lysozymesbind to theaptamer-modified gold electrode, the surface density of electrostatically bound $[Ru(NH_3)_6]^{3+}$ decreases, leading to the decreased CV peak current.

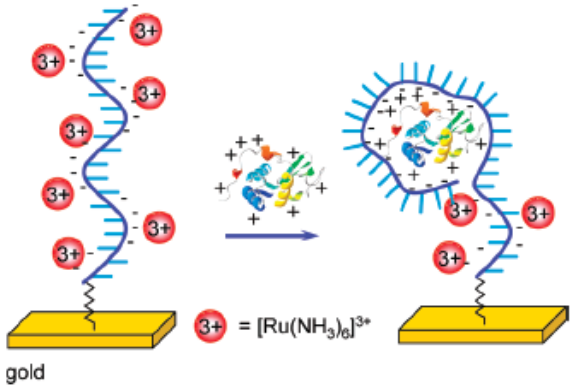

Figure 1-9. Aptamer-based biosensors with solution-diffused redox makers.

Note: Yu (2007); used with permission

Methylene blue (MB), a DNA intercalator, also has been used as a solution-diffusedredox marker to detect thrombin.[38] A piece of DNA containing anti-thrombin DNA aptamer can fold to a hair-pin structure and then become immobilized ona gold electrode. Prior to incubation with thrombin, methylene blue in solution is supposed to intercalate with the double-helical stem of the hair-pin structure. Then a smaller peak current is observed after incubation with thrombin. Bang et al.[38]proposed that the thrombin-induced conformational change would causethe dissociation of the double-helical section anddecrease the amount of methylene blue on the electrode surface.

Consequently, a smaller peak current should be observed in this case. In fact, the interaction between methylene blue and DNA is rather complex, as discussed below.

1.4. **Methylene blue and its interaction with DNA**

Methylene blue (MB) belongs to the phenothiazine family with a structure shown in Figure 1-10.It usually exists in its salt form,methylene blue chloride. The solution of MB appears blue since it has an excitation wavelength around 650 nm with a high excitation coefficient.[39, 4]

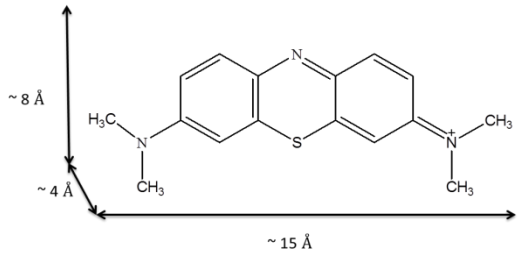

Figure 1-10. Molecular structure of methylene blue and its dimension.

MB is widely used in many fields including medicine, chemistry, and biology. For example, during surgeriesMB can be used to visually trace lymphatic drainage or to test the urinary tract.In chemistry,MB can be used as a redox titration indicator since the solution of its reduced form, leucomethylene blue (LB), is colorless. It has been generally accepted that MB would undergo a reversible one-proton coupled two-electron reduction process around neutral pH to form leucomethylene blue (as illustrated in Figure 1-11).[41]

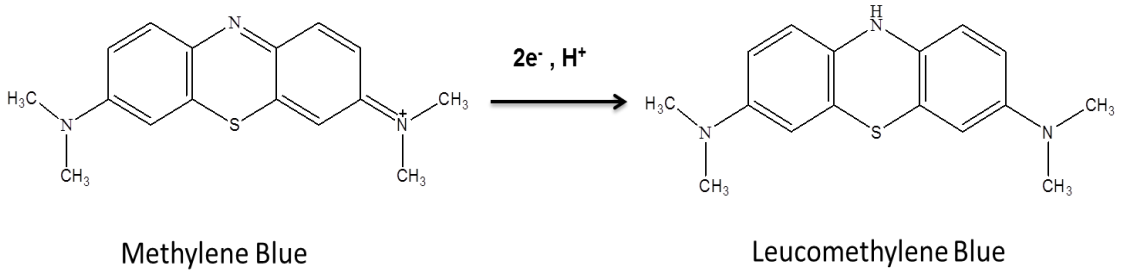

Figure 1-11. Reduction of methylene blue at neutral pH.

In biology, MB is extensively used as an optical probe of nucleic acids, chromatin and nucleosomes; thus researchers investigated binding modes of the MB-DNA interaction.[42-48]. Generally speaking, four bindingmodes of MB-DNA have been proposed and supported experimentally. They include a) intercalation, b) major groove binding, c) electrostatic binding and d) single-guanine specific base stacking.

As mentioned in ***1.1.1.***, like many other proflavins, positively charged methylene blue can replace counter ions (e.g. Na^+) and electrostatically bind to DNA.[5]Intercalation of methylene blue has been discussed since 1970s;Bradley et al. used electro-optical measurements to show that MB in the MB-DNA complex is perpendicular to the helix.[45]Norden et al. extensively used circular dichroism and linear dichroism to study the MB-DNA interaction and they concluded that (a) intercalation is the only binding mode of MB to both the alternating [poly-(dG-dC)]$_2$ (750 b.p.) and non-alternating poly(dG)•poly(dC) (8560 b.p.), and the mode of binding here is insensitive to the ionic strength; (b) intercalation is a major binding mode of MB to alternating [poly(dA-dT)]$_2$ (2658 b.p.) at low ionic strength, while major groove bonding may become dominating at high ionic strength; (c) major groove bonding may be the only binding mode for MB with non-alternating poly(dA)•poly(dT) (349 b.p.) and (d) for a calf-thymus DNA (42%GC), at low ionic strength (below 0.2 M), methylene blue prefers to intercalate at GC sites while

at high ionic strength (above 0.2 M) it prefers AT sites, and both intercalation and major groove binding modes can be expected.[43,44]

Gooding et al. found that the CV peak current generated from methylene blue bound to ssDNA-modified electrodes increased with guaninecontent, indicatingthat methylene blue could bind to a single guanine base specifically.[47]According to molecular dynamic simulations, Enescu et al. proposed a “stacking” conformation for the structure of guanine-MB complexes in water, and the free energy change of MB-guanine complex formation was calculated to be -7.2±0.2 kcal/mol.[48]

All the above binding modes involve the most basic types of interaction in a biomolecular system such as electrostatic force governed by Coulomb’s Law, van der Waals force combining London dispersion and exclusion, and hydrogen bonding. In summary, MB-DNA intercalationisDNA sequence and ionic strength dependent; an apparent overall dissociation constant for methylene blue with calf-thymus DNA in solution was measuredto be 46 M.[46] Further detailed research on MB-DNA interactions is necessary, although researchers already widely use methylene blue as a redox marker to develop“label-free” electrochemical biosensors. Besides Bang and coworkers who used methylene blue as redox marker to detect thrombin, others were interested in using it to differentiate between ssDNA and dsDNA, simply via electrochemicalcharacterizations (e.g. peak current and formal potential).[90]

1.5. **Research objectives and outline**

Firstly, we aimed for thedevelopment of a simple yet sensitive version of “label-free” electrochemical biosensors for small molecules (e.g., adenosine);we planned

toimmobilize the“integrated ligand sensor” (Figure 1-5)on gold electrodes through Au-S bonding; then we would use solution-diffusedmethylene blue as redox marker to examine possible conformational changesinduced by the target (adenosine) binding. Secondly, by making a comparison between the “integrated ligand sensor” and a fully complementarydsDNA, wehoped to achieve a deeper understanding of the MB-DNA interactions and the signallingmechanism. Thirdly and more importantly, we wantedto study fundamental aspects of methylene blue redox behaviour with bare gold electrodes and electrodes modified with alkanethiols. This is important because for a “label-free” electrochemical biosensor, in which alkanethiols are used as spacers;methylene blue in solution maysimply be trapped by this spacer layer. In the following sections, I will first describe our study of the MB redox behaviouron bare and SAM-modified gold electrodes, and then discussmy investigations of the different interaction modes between MB and the “integrated ligand sensor”construct, as well as its comparison with fully complementary dsDNA.

2. ExperimentalSection

Materials and procedures for the experiments are described in this section. Basic electrochemical data processingprocedures are also provided.

2.1. **Materials**

All reagents were obtained in their highest available purity and used without further purification unless otherwise noted.Potassium ferricyanide(III) ($K_3Fe(CN)_6$) (99.99%), hexaammineruthenium (III) chloride ($Ru(NH_3)_6]Cl_3$) (98%), methylene blue chloride (98%),11-mercapto-1-undecanol (97%), 11-mercapto-1-undecanoic acid (95%), 6-mercapto-1-hexanol, adenosine, and lithium chloride (LiCl) were obtained fromSigma-Aldrich (Oakville, ON). Adeninemonophosphate (AMP), uracil monophosphate (UMP), and guanine monophosphate (GMP) wereprovided by Dr. Sen.Magnesium chloride hexahydrate ($MgCl_2•6H_2O$) was purchased from EM Science (Gibbstown, NJ), EDTA disodium dihydrate from Bishop (Burlington,ON), Tris(hydroxymethyl) aminomethane (Tris) from Caledon Laboratories Ltd. (Georgetown, Ontario)

Both HPLC-purified thiol-modified and unmodified DNA oligonucleotides were purchased from Biosearch Technologies (Novato, CA). After reducing the disulfide bond of the modified ssDNA (strand 1) (as shown in Figure 2-1), the activated strand 1 was hybridized with unmodified ssDNA (strand 2 or 3) to formthe dsDNA-aptamer constructs(apt-DNA) or a fully complementary DNA duplex (comp-DNA), respectively.

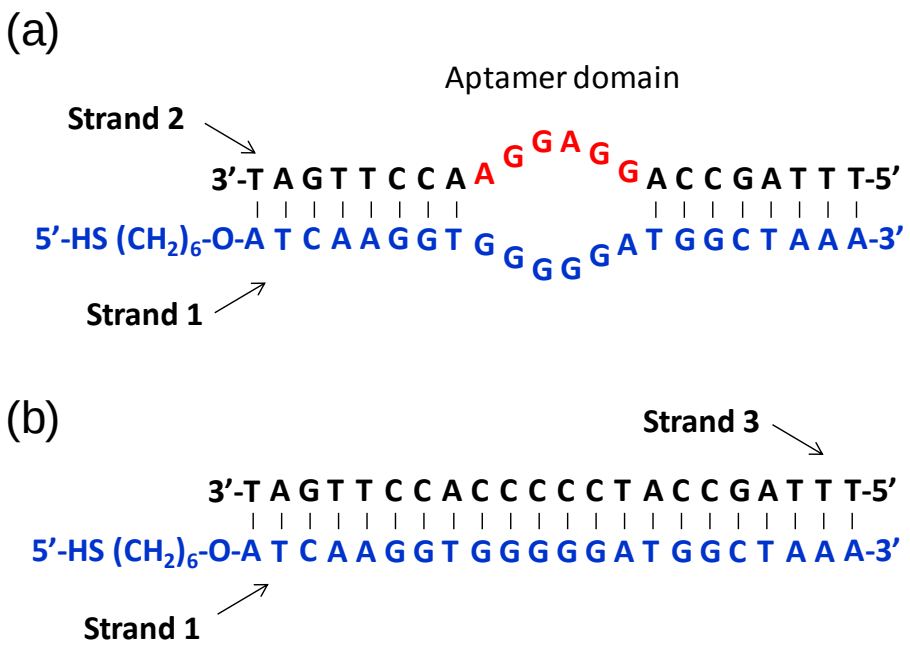

Figure 2-1. ***Illustration of the secondary structure of (a) the dsDNA-aptamer construct (apt-DNA) and (b) the complementary DNA duplex (dsDNA).***

Gold substrates (100 nm Au/5 nm Cr/glass) were purchased from Evaporated Metal Films Inc.(Ithaca, NY); illustra^{TM}Microspin^{TM} G-50 columns were purchased from GE healthcare (Buckinghamshire, UK);de-ionized water (>18.3 MΩ cm) from a Barnstead Easy Pure UV/UF compact water system (Dubuque, IA) was used in all experiments. pHValues for the buffers were measured with a pH meter (35617 Series, OAKTON). All plastic ware was pre-siliconized.

2.2. **Experimental procedures**

2.2.1. Preparation ofbare and SAM-modifiedgold electrodes

Gold chips (2.5 cm x 1.5 cm) were cut from a gold slide(2.5 cm × 7.5 cm), cleaned with freshly prepared piranha solution [3:1 (v/v) mixture of concentrated

$H_2SO_4$and 30% H_2O_2 (WARNING: piranha solution reacts violently with organic solvents and must be handled with extreme care)] at 90 ºC for 5 minutes, rinsed thoroughly with de-ionized water and the extra water on the surface removed with compressed N_2 gas. These freshlyprepared gold chips are ready to be used as working electrodes for testing MB electrochemistry or to be subsequently modified with alkanethiols.

Stock solution of alkanethiols, 11-mercapto-1-undecanol (97%), 11-mercapto-1-undecanoic acids (95%), 6-mercapto-1-hexanolwould be diluted to 1 mM with ethanol (95%) or de-ionized water (11-mercapto-1-undecanol barely dissolves in de-ionized water; hence ethanol (95%) was used as solvent).Alkanethiols were immobilized on cleaned gold chips by spreading a 200- L droplet of the diluted solution for 15 hours at 100% humidity or 100% ethanol-saturatedenvironment (for 11-mercapto-1-undecanol).Prior to the electrochemical measurements, all these modified gold chips were stored inde-ionized buffer orethanol (95%)at room temperature.

2.2.2. Preparation of the DNA constructs in solutionand gel assay

For the biochemical test, the dsDNA-aptamer construct (i.e., the DNA construct that incorporates the anti-adenosine aptamer, apt-DNA) and the complementary DNA duplex (dsDNA) were formed by annealing equimolar mixtures (2 µM each) of the constituent strands in a binding buffer (10 mMTris-HCl, 150 mMLiCl, 3 mM $MgCl_2$, 0.1 mM EDTA, pH 8.2). The mixture was heated to 80 ºC for 5 min, and then cooled slowly to room temperature; 12% non-denaturing gel was run to confirm the formation of the apt-DNA and dsDNA with and without adenosine by comparing the gel mobility with that of each ssDNA. A 19:1 acrylamide-bisacrylamide solution was used as stock solution. The loading volume of each individual lane was 10 L. The gels were run in a SE600

Series Standard Vertical Electrophoresis Unit at 300 V for 1.5 hour. Bromophenol Blue and Xylene Cyanol FF were gel loading dyes to track the positions of the DNA strands on the gel. After running, the gels were stained with ‘‘stains all” solution for 2 hours and destained before scanning.

2.2.3. Preparation of DNA-modified gold electrodes

A 4-hour incubation of the thiol-modified ssDNA (strand 1) with 10 mMtris(2-carboxyethyl)phosphine hydrochloride (TCEP, Sigma-Aldrich) in the binding buffer (pH 8.3) was necessary to activate this ssDNA by reducing the disulfide bond. By varying the initial amount of strand 1 (see Figure 2.1), we were able tocontrol the surface density of double strand DNA (both apt-DNA and dsDNA) on the gold electrode. A MicroSpin^{TM} G-50 column, rinsed with deoxygenated binding buffer prior to use, was used to remove impurities. Then the concentration of the purified strand 1 was measured with a Nanodrop ND-1000 spectrophotometer (Davis, CA). Equal amounts of strand 2 or 3 were added to strand 1, followed by annealing to form apt-DNA and dsDNA, respectively. A 20-µl droplet of apt-DNA or dsDNA was then immediately spread on the surface of the cleaned gold chip and let the droplet cover the central part of the gold chip, and the DNA-coated chips were stored in a box at 100% relative humidity at room temperature for 15 to 30 hours. After DNA immobilization, a one-hour incubation of 1 mM 6-mercapto-1-hexanol was applied to passivate the gold surface and remove non-specifically adsorbed DNA. Finally, the gold chips were rinsed thoroughly with 10 mMTris-HCl buffer (pH 8.2). Prior to the electrochemical measurements, all the modified gold chips were stored with binding buffer in a box with 100% relative humidity at room temperature.

2.2.4. Electrochemical measurements

Electrochemical experiments were carried out using a 10-ml three-electrode cell. The cell was constructed with a circular hole at the bottom to expose the workingelectrode; the reaction area of the working electrode was restricted to 0.66cm^2 by a polytetrafluorethylene O-ring. An Ag | AgCl | 3M NaCl reference electrode and a Pt wire counter electrode were used for all the measurements.

2.2.4.1. Electrochemical measurementswith bare gold electrodes

A cleaned bare gold chip was used as the working electrode. Electrochemicalmeasurementswere performedwith a CHI1040A Electrochemical Analyzerin a Faraday cage at room temperature. Electrolytes (10 mMTris-HCl, 150 mMLiCl, 3 mM $MgCl_2$, and 0.1mM EDTA) at different pH values (1.8, 5.3, 7.3, 8.3, 10.9, and 12.1)were tested,respectively. Stock solution of methylene blue was shielded from light and used to prepare micromolar range solutions.In order to study the redox behaviour of the adsorbedMB, the electrodes were incubated with 1 mM methylene blue for 15 hours, then gently washed with deionized water and tested inMB-free electrolytes.

2.2.4.2. Electrochemical measurements with alkanethiolate SAM-modified gold electrodes

An alkanethiol-modified gold chip was used as working electrode. These electrochemicalmeasurements were performed with a CHI1040A Electrochemical Analyzer in a Faraday cage at room temperature. Electrolytes containing 10 mMTris-HCl, 150 mMLiCl, 3 mM $MgCl_2$ and 0.1 mM EDTA, at pH 7.3wereused; stock solutions of methylene blueandferric cyanide were shielded from light and used to prepare micromolar rangesolutions for electrochemical measurements. In order to study the redox behaviour of surface-confined MB, electrodes were incubated with 1 mM

methylene blue for 15 hours, then gently washed with deionized water and tested inMB-free electrolytes.

2.2.4.3. Electrochemical measurementswith DNA-modified gold electrodes

An apt-DNA or ds-DNA modified gold chip was used as working electrode. The electrochemicalmeasurements were performed withμAutolab IIpotentiostat/galvanostat(Eco Chemie B.V. Utrecht, The Netherlands). Stock solutions of methylene blueandferric cyanide were shielded from light and used to prepare micromolar range samplesolutions for electrochemical measurements. Stock solution of hexammineruthenium (III) chloride was stored at – 4ºC and added directly to the cell for measurements. Tris buffer (10 mMTris-HCl, pH 8.2) was used as electrolyte for measurements of hexammineruthenium (III). Binding buffer (10 mMTris-HCl, 150 mMLiCl, 3 mM $MgCl_2$, 0.1 mM EDTA, pH 8.2) was used as electrolyte for measurements inferric cyanideand methylene blue solutions.

The cathodic peak of the first scan at 0.5 V/s of $Ru(NH_3)_6]Cl_3$ was integrated to determine the DNA surface density on gold.[49,50]Prior to determining the MB surface density, the $[Ru(NH_3)_6]Cl_3$in the cell was removed by gentle washing with Tris buffer followed by incubation with binding buffer for 20 minutes.[51]The cathodic peak of MB at 0.1 V/s after 30 minutes equilibration was used to determine the surface density of MB before and after adding adenosine.The incubation time of adenosine was fixed at 15 hours. In the test of selectivity, the incubation times of AMP, GMP, UMP and the blank were also 15 hours. The removal of AMP and adenosine was carried out by gently washing the electrode with binding buffer three to five times and incubating with binding buffer for at least 20 minutes. A stable CV after removing each target would be used as background for the following tests.

2.3. **Electrochemical Data Processing**

2.3.1. Determination of the DNA surface density

Surface densities of any surface-adsorbed redox-active species (e.g. MB, $[Ru(NH_3)_6]Cl_3$) can be obtained by integrating the reduction peak of theirrespective CVs, assuming that all surface-bound MB or $[Ru(NH_3)_6]Cl_3$is electroactive:

$$\Gamma_o = \frac{Q}{nFA} \quad \text{(Equation 2-1)}$$

where Q is the integrated charge of the cathodic peak, *n* is the number of electrons transferred, *A* is the electrode area, *F* the Faraday constant.

The surface densityof dsDNA was measured by our previously reported protocol.With 3.5 μM $Ru(NH_3)_6^{3+}$ added to the electrolyte, we can obtain reversible CVs of the $Ru(NH_3)_6^{3+}$ electrostatically bound to the DNA-modified electrodes.[49,50]The surface density of DNA constructs is then calculated by using Equations 2-2 and 2-3.

$$Q = nFA\Gamma_{\mathrm{Ru}} \quad \text{(Equation 2-2)}$$

$$\Gamma_{\mathrm{DNA}} = \Gamma_{\mathrm{Ru}} \frac{Z}{m} N_A \quad \text{(Equation 2-3)}$$

where*Z* is the charge of the redox molecules ($Ru(NH_3)_6^{3+}$) and *m* is the number of nucleotides.

2.3.2. The homogeneous electron transfer rate constant

Laviron's theory has been widely applied to determinethe homogenous electron transfer rate constant of a surface-adsorbed species.[52]

$$E^{o'} - E_{pa} = \frac{RT}{(1-\alpha)nF} ln\text{?} + \frac{RT}{(1-\alpha)} ln\left(\frac{(1-\alpha)nF}{RT\kappa}\right) \quad \text{(Equation 2-4)}$$

$$E^{o'} - E_{pc} = \frac{RT}{\alpha nF} ln\text{?} + \frac{RT}{\alpha} ln\left(\frac{\alpha nF}{RT\kappa}\right) \text{(Equation 2-5)}$$

Equations 2-4 and 2-5 derived by Lavironexpress well the relationship between$E^{o'}$- E_{pa} or $E^{o'}$- E_{pc} versus scan rate ( ). By making a plot of$E^{o'}$- E_{pa} or $E^{o'}$- E_{pc} versusln( ), one obtains a straight line in thehigh scan rate region in which E_{pa}–E_{pc} is greater than$\frac{200\ mv}{n}$ (n = 2 for methylene blue) (see Figure 4-5).[52]After finding the slope and intercept of this straight line, we can calculate the homogenous electron transfer rate constant from the above equations.

2.3.3. The heterogeneous electron transfer rate constant

Nicholson first proposed that cyclic voltammetry is a feasible and promising method to estimate the apparentheterogeneous electron transfer rate constant.[53] His breakthrough work offered a model for extractingimportant parameters from CV data. According to his theory, we need first to find $\Delta E_p \times$ n, where n is the number of transferred electrons and $\Delta E_p = E_{pa} - E_{pc}$. Then we can easily look up a correspondingψ value in his simulation model and subsequently we can find the apparent electron transfer rate constant, once the diffusion constant is known (the simulation curve is shown in Figure 2-2).

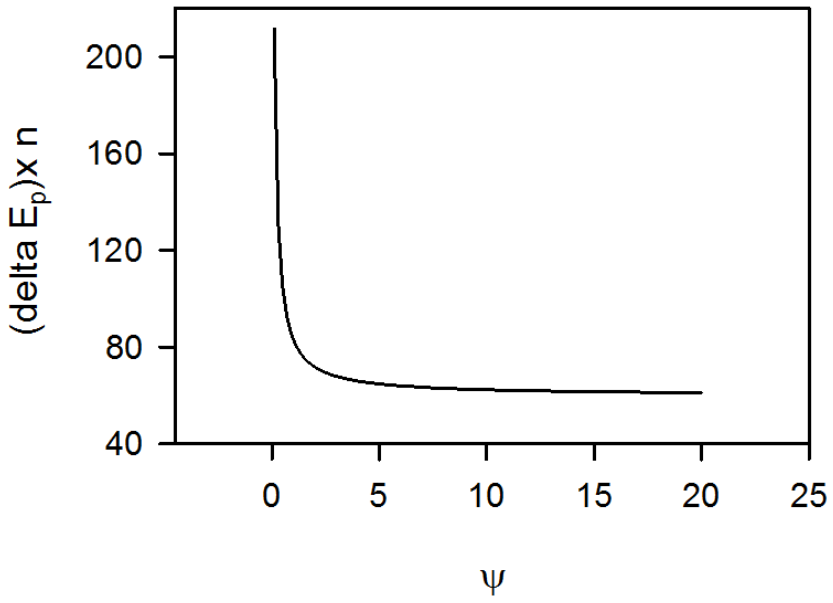

Figure 2-2. ***Simulation curve to determine the heterogeneous electron transfer rate constant. "deltaE$_p$" means E$_{pa}$–E$_{pc}$; n is the number of electrons transferred; ψ is the parameter to be estimatedwhen delta E$_p$ is read from a CV. Ψ then is further used to determine the heterogeneous electron transfer rate constant when the diffusion coefficient is known.***

Note: Please see reference 53 more detail.

3. Behaviour of methylene blue on bare gold or alkanethiolate SAM-modified gold surface

In this section, I will describe the electrochemical studies of solution-diffused MB on both bare and alkanethiolate SAM-modified gold electrodes; the electrochemicalfundamental research on how methylene blue behaves on bare gold electrode and on alkanethiol-modified gold electrodes is necessary; it would be beneficial for us to deep understand our “label free” electrochemical biosensor later. Herein, thebehaviour of methylene blue on bare gold and on alkanethiol-modified gold surfacesis discussed.

3.1. Redox behaviour of methylene blue with bare gold electrode

Methylene blue was originally used as indicator in redox titrations.Its redox properties have been characterized with various working electrodes including mercury electrodes, sulphur-modified gold electrodes, andplatinum electrodes.[54-56] Previous studies have shown that methylene blue can undergo a two-electronreduction to leucomethylene blue (Figure 1-9).Figure 3-1 shows a representative CV plot of MB on a bare gold electrode. At a scan rate of10 mV/s,it was observed that (a) the anodic and cathodic peaks are symmetric and the ratio of anodic to cathodic peak current (i_{pa}/i_{pc}) is close tounity; (b) the peak potential separation, ΔE (i.e.,E_{pa}-E_{pc}) is 29.0 mV.

$$E_{pa} - E_{pc} = 2.2\frac{RT}{nF} = \frac{56.5}{n}\ mV\ at\ 25\ ℃ \qquad \text{(Equation 3-1)}$$

If we apply Equation 3-1, a convenient “diagnostic tool” for a reversible wave[57] and assume that it is a two-electron transfer process, the experimental result (29.0 mV) is very close to the theoreticalΔE (28.0 mV at 22°C).

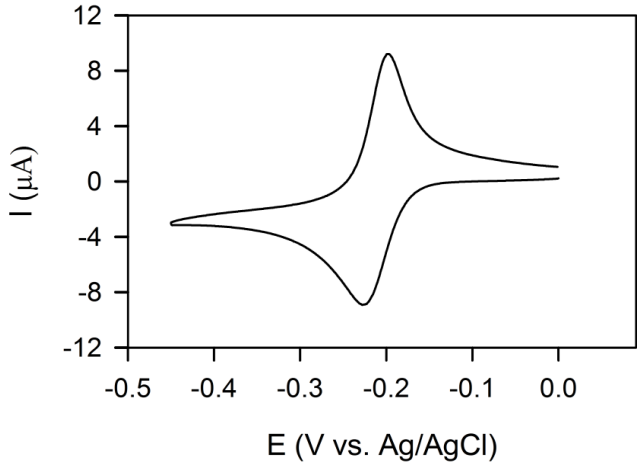

Figure 3-1. A representative CV of 100 μM MB on gold electrode; the electrolyte solution consists of 150 mMLiCl, 10mMTris, 3mMMgCl$_2$, pH = 7.4. The scan rate is10 mV/s.

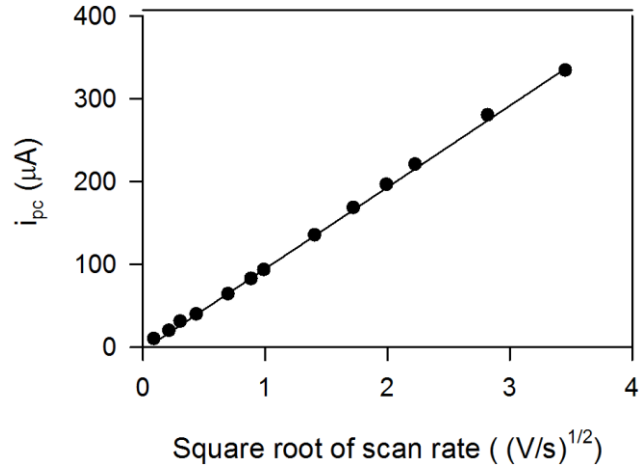

Figure 3-2. Scan rate dependenceof the CV reduction peak current of 100 μM MB on gold electrode in 150 mMLiCl, 10mMTris, 3mM MgCl$_2$, pH = 7.4)

Figure 3-2 shows a linear relationship between the reduction peak current and the square root of the scan rates when the bulk concentration of methylene blue is high (100

M).Equation 3-2 predicts such a linear relationship for a reversible system, consideringthe diffusion of redox speciestoward the electrode.

$$i_p = 0.4463nFAC_o^* \left(\frac{RT}{nF}\right)^{1/2} v^{1/2} D_o^{1/2} \quad \text{(Equation 3-2)}$$

The diffusion coefficient can be estimated from Equation 3-2, where A is the electrode surface area (in cm^2); D_o is the diffusion coefficient (in cm^2/s); is the scan rate (in V/s); n is the number of transferred electrons. The thus determined D_o of methylene blue is 8.9 x 10^{-6} cm^2/s, which is close to the value reported by Bardeleben.[58] Using the methodology developed by Nicholson,[53] we can estimate the apparentheterogeneouselectron transfer rate constant (κ) via CV measurements (see Appendix C); the κvalue was determined to be 10.6 cm/s.The above observation confirmed that the redox reactionof methylene blueat neutral pH is a two-electron process; when the bulk concentration is high, this process is diffusion-controlled and reversible.

3.1.1. The pH dependence of the MB redox process

Previous studieshave revealed that the redox process of methylene blue is proton-coupled;Figure 3-3 shows that the formal potential indeed increases with decreasing pH value. This shift is predicted by Equation 3-3.

$$E^{\circ\prime} = E^{\circ} - \frac{0.5916}{2}\log\left[\frac{\alpha(LB)}{\alpha(MB^+)\alpha(H^+)}\right] \quad \text{(Equation 3-3)}$$

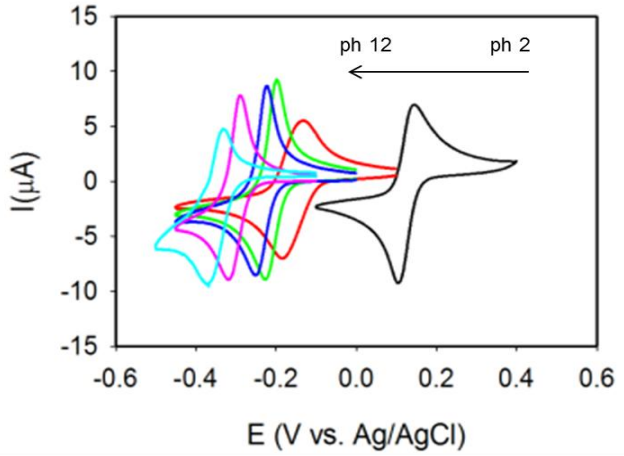

Figure 3-3. CVs of 100 μM MB on bare gold electrode in 150 mMLiCl, 10mMTris, 3mM $MgCl_2$, pH = 2 - 12; scan rate = 10 mV/s.

Hence wecan also expect a linear relationship between the formal potential and the pH value, and Figure 3-4 shows such a linear relationshipat pH 7-12 with a slope of-0.0275 V/pH, which is close to the theoretical value (-0.0296 V/pHbasedon Equation 3-3). This confirms that from pH 7 to pH 12 the redox process of methylene blue is a one-proton coupled reaction.

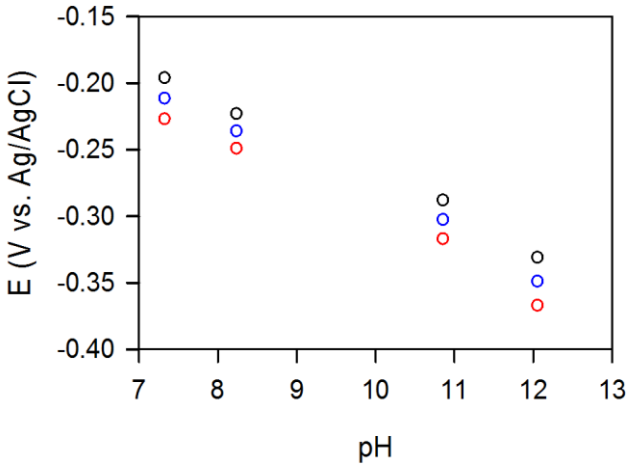

Figure 3-4. pH dependence of formal potential (blue circles), cathodic peak potentials (black circles) and anodic peak (red circles) potentials.

Besides a linear relationship between the formal potential and pH values, a linear relationship is also observed between cathodic peak potentials (or anodic peak potentials) andpH values. Moreover, such linear relationships show that slopes are close to each other (dE_{pa}/pH = -0.0288 V/pH; dE_{pc}/pH = -0.0277 V/pH; $dE^{o'}$/pH = -0.0275 V/pH). This indicates that inthis pH range (7 -12), protonation doesnot affect the reduction and oxidation process of methylene blue. In the study of the redox behaviour ofazobenzene SAMs on gold.[59] Yuet al. found thatthe formal potential, anodic peak potential and cathodic peak potential alsoshow linear relationships with pH values; however, the differencebetween the slopes is relatively large, indicating that deprotonation in the anodic process of azobenzeneis hindered by kinetic factors. Figure 3-5 shows that the slope of the $E^{o'}$-pH linear relationship is almost independent on the scan rates, indicating that the protonation and deprotonation processes of methylene blue exist in a fast equilibriumwithin the time scale of electrochemical measurements.

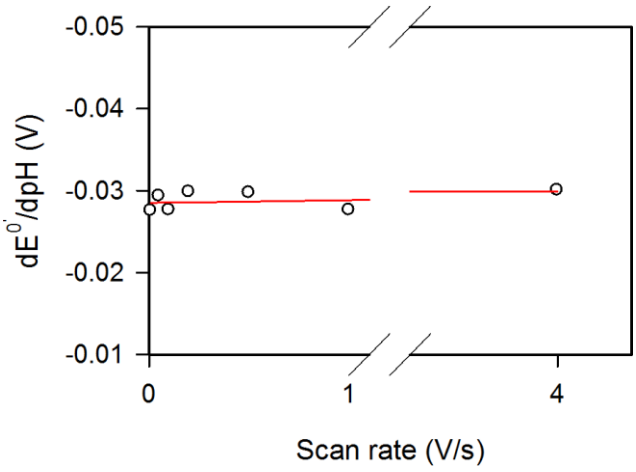

Figure 3-5. Variation of $dE^{o'}/dpH$ as function of scan rate; 100 µM MB on gold electrode in 150 mMLiCl, 10mMTris, 3mM $MgCl_2$, scan rate = 10, 50, 100, 200, 500, 1000, 4000 mV/s.

Although protonation-deprotonation is a fast equilibrium when methylene blue undergoes the redox process, the pH value does affect the apparentheterogeneouselectron transfer rate constant (κ). Figure 3-6 shows that at high pH, the apparent electron transfer rate constants are larger than that in thelower pH range. Laviron has shown that the variations of the apparentheterogeneous electron transfer rate constants (κ) are determined by the detailedredoxmechanism. For a two-electron one-proton redox process, the mechanismmay be EEC, ECE, or

$O^+ \overset{e^-}{\leftrightharpoons} R\bullet^+ \overset{e^-}{\leftrightharpoons} R^- \overset{H^+}{\leftrightharpoons} R$ EEC mechanism

$O^+ \overset{e^-}{\leftrightharpoons} R\bullet^+ \overset{H^+}{\leftrightharpoons} RH^+ \overset{e^-}{\leftrightharpoons} R$ ECE mechanism

$O^+ \overset{H^+}{\leftrightharpoons} OH^{2+} \overset{e^-}{\rightleftharpoons} OH^+ \overset{e^-}{\leftrightharpoons} R$ CEE mechanism

CEE.

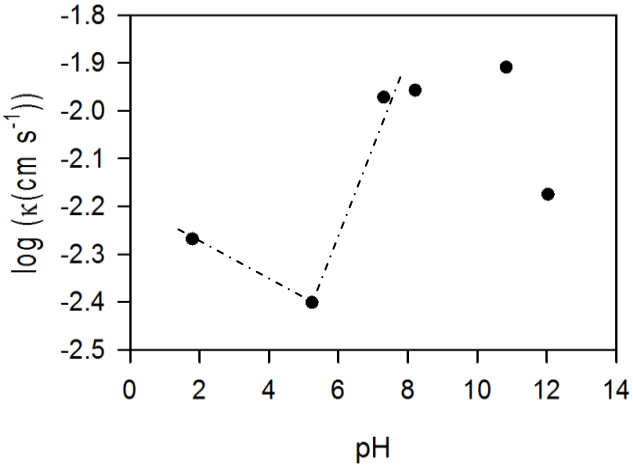

Figure 3-6. Variation of log(κ) as a function of pH

At high pH (low proton concentration), the EEC mechanism would be the major process and κ is relative large; at medium pH, ECE would be more favoured than the others and κ is relatively small; whenthe proton concentration is high, the CEE mechanism would be the dominating one and κ becomes large again. Figure 3-6 shows such a V-shape curve, which indicates that the reduction of methylene blue undergoes an ECE mechanism at medium pH. The *in-situ* electrochemical EPR study by Dong and co-workers in fact supported such a hypothesis;[60]they also identified the radical intermediate during the reduction process of methylene blue.

3.1.2. The adsorption of methylene blue on bare gold

An interesting phenomenon was found on examination of the scan rate dependence of the CV plots of solution-diffused methylene blue on bare gold electrodes. Ata low scan rate, in terms of the peak current, the cathodic and anodic peaks are symmetric. However, when the scan rate was increased, the ratio of anodic peak current to cathodic peak current increased to around 1.5. (Figure 3-7)

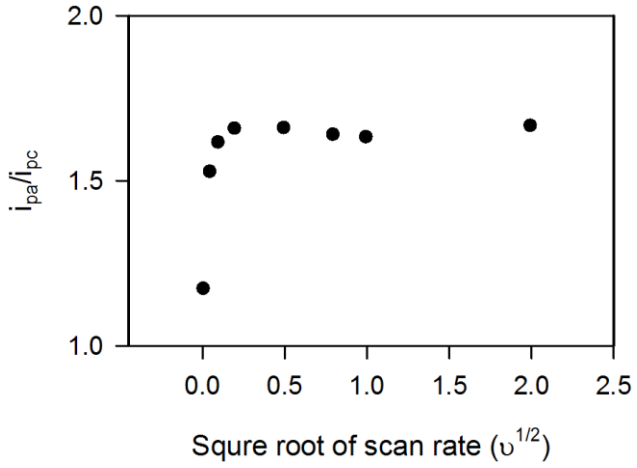

Figure 3-7. Variation of peak current ratio with scan rate for CV of solution-diffused methylene blue.

Wopschall and Shain have studied this phenomenon both by experiments using mercury drop electrodes and by numerical simulations.[61-62]They have found that if the redox products (R) can weakly adsorb on the electrode surface, then with increasing scan rate, the anodic peak current (from the oxidation of the products) would increase more than the cathodic peak current. This difference can also be explained byexamining thefollowing fundamental electrochemistry equations.

$$i_p = \frac{n^2F^2}{4RT} vA\Gamma \quad \text{(Equation 3-4)}$$

$$i_p = 0.4463nFAC_o \left(\frac{nF}{RT}\right)^{1/2} v^{1/2} {D_o}^{1/2} \quad \text{(Equation 3-5)}$$

Equation 3-4 shows how the peak currents of redox species immobilizedon an electrode surface depend on the scan rate. The peak current of a surface-immobilized species is directly increasing with the scan rate. Meanwhile, according to Equation 3-5, which describeshow peak currents of solution-diffused species change with the scan rate, the peak current is proportional to the square root of the scan rate. Hence, the peak current of absorbed species would increase faster than that of solution-diffused species when

the scan rate is increased. Wopschall and Shain simulated a cyclic voltammogram of a redox species whose reduced product isweekly adsorbed on the electrode surface; our CV of solution-diffused methylene blue (Figure 3-8) sharessimilar characteristicswiththeir simulation.[61]

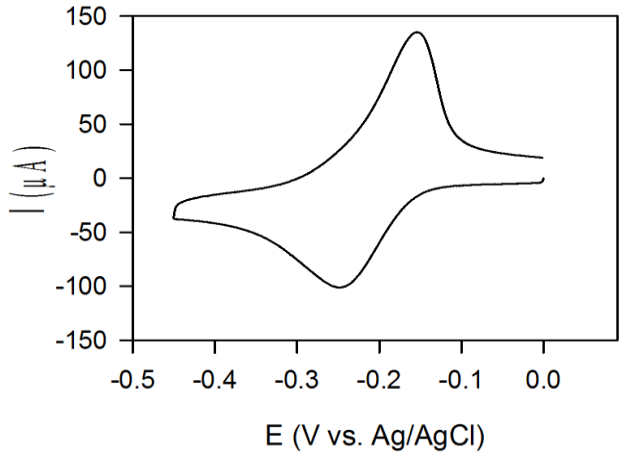

Figure 3-8. CV of 100 μM MB on gold electrode in 150 mMLiCl, 10 mMTris, 3 mM $MgCl_2$, pH = 7, at a high scan rate (1 V/s).

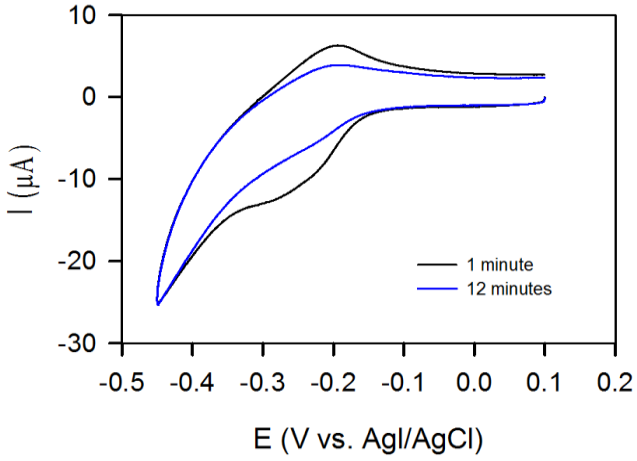

Figure 3-9. CV of surface-adsorbedMB with gold electrode in the electrolyte (150 mMLiCl, 10 mMTris, 3 mM $MgCl_2$, pH = 7; scan rate = 100 mV/s).

Therefore, it is reasonable to believe that the reduced form of methylene blue, leucomethylene blue,isweakly adsorbed on the electrode surface. Moreover, I also found that methylene blue itself adsorbs on the electrode surface. If a clean gold electrode was immersed in a solution containing 1.0mM methylene blue for a long time (15 hours), after gently washing, clear-cut redox peaks are observed when the electrode is placed in a MB-free electrolyte. The peak current gradually decreases, indicating that originally surface-adsorbed methylene blue were movingfrom the surface to the solution. This process is rather fast; about 80% surface-adsorbed methylene blue would movefrom the surface tothe solution in the first two minutes and only around 7% would remain on the surface at equilibrium. The homogeneous electron transfer rate constant of this surface adsorbed methylene blue was estimated to be 267 s^{-1} using Lavrion's method.

3.2. **Redox behaviour of methylene blue on a gold electrodemodified with 11-mercapto-1-undecanol**

11-Mercapto-1-undecanol (MCU)has been studied as a model system for investigating SAM formation on gold substrates.[63]Lee and coworkers have systematicallyexamined the adsorptionbehaviour of 11-mercapto-1-undecanol using*in-situ*scanningtunnelling microscopy (STM) and cyclic voltammetry. They found that when the concentration of 11-mercapto-1-undecanol is low (less than 50 μM), it can initially adsorb on the gold surface in a “flat-lying” phase and gradually reorient into a “standing-up” phase with a molecular arrangement of $(\sqrt{3}x\ \sqrt{3})R30^{o}$. At a high concentration of 11-mercapto-1-undecanol, the molecules can directly form the “standing-up” phase in half an hour.

At the early stage of SAM studies, researchers examined heterogeneous electron transfer processes of different redox active species at alkanethiolate SAM-modified gold electrodes. Groat et al. argued that the surfacecharge is a determining factor in the heterogeneouselectron transfer kinetics, and they used ferrocene as the redox probe to probe SAMdefects .[64]Finklea and coworkers pointed out that the pinholes (defects) in the monolayers play an important role in the electron transfer kinetics.[65]Unlikeferrocene, methylene blue is barely blocked by alkanethiolateSAMs on the gold electrode, which triggered Nakashima’s interest in this topic.[66]

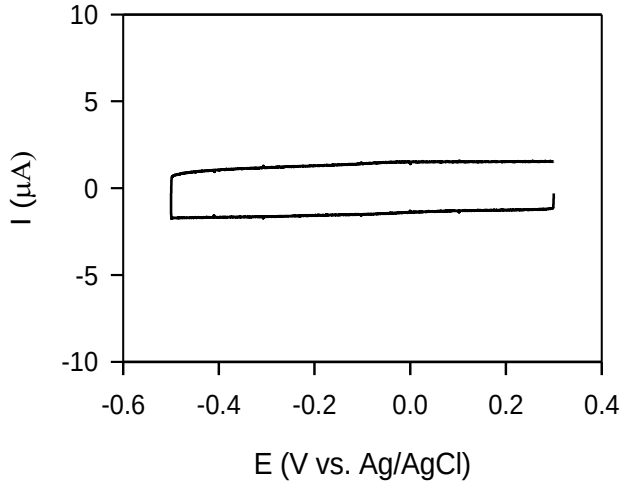

Figure 3-10. CV of 11-mercapto-1-undecanol SAM-modified gold electrode in 150 mMLiCl, 10mMTris, 3mM $MgCl_2$, pH = 7.4; scan rate = 1V/s

As shown in Figure 3-10, no redox peaks can be found in the range from -0.5 V to 0.4 V (vs. Ag/AgCl), when performing CV scans in the absence of any redox molecules in the electrolyte; rather it shows the typical capacitance (charging) current.

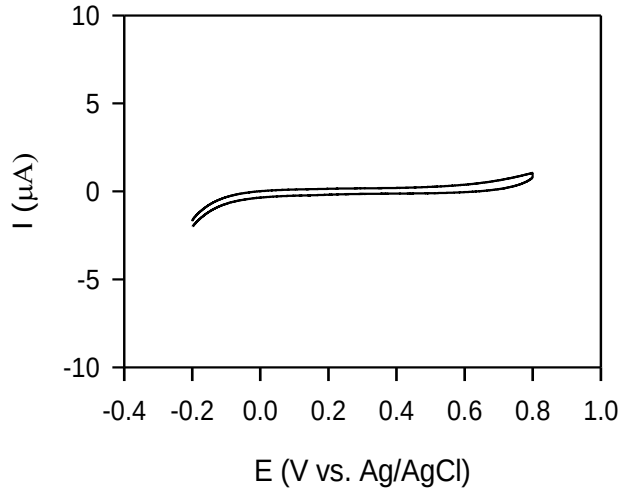

Figure 3-11. CV of 100 μM $K_3Fe(CN)_6$on11-mercapto-1-undecanol-modified gold electrode in salt buffer (150 mMLiCl, 10mMTris, 3mM $MgCl_2$, pH = 7.4); scan rate = 100 mV/s

Figure 3-11 shows theCV of solution-diffused$K_3Fe(CN)_6$on gold electrode modified with11-mercapto-1-undecanol SAM. As expected, the reduction of $Fe(CN)_6^{3-}$is

completelyblocked and no redox peak of $Fe(CN)_6^{3-}$isobserved. This result confirms that a relative densely packed SAM was formed on the gold electrode.

Figure 3-12 is a typical CV of solution-diffused methylene blue onan 11-mercapto-1-undecanol-modified gold electrode. Compared with Figure 3-11 (CV of$K_3Fe(CN)_6$), Figure 3-12 shows a clear pair of redox peaks. In contrast to Figure 3.1 (MB on bare gold electrode), the CV in Figure 3-12 presents a much larger peak separation. The apparentheterogeneous electron transfer rate constant was estimated at 0.8×10^{-3} cm/s, which is only one-tenth of that of methylene blue with a bare gold electrode. This result confirmed that solution-diffusedmethylene blue can penetrate the SAM, but the apparent electron transfer (which may be limited by the diffusion kinetics) was blocked by the SAM.[67]

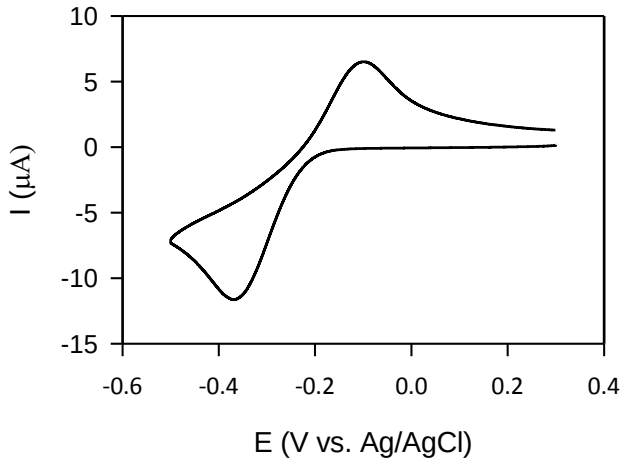

Figure 3-12. CV of 100 µM MB on11-mercapto-1-undecanol-modified gold electrode in 150 mMLiCl, 10mMTris, 3mM $MgCl_2$, pH = 7.4); scan rate = 100 mV/s.

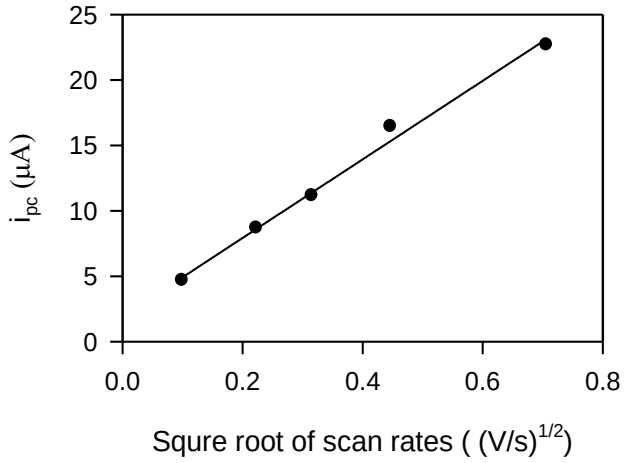

Figure 3-13. Peak current of the CV shown in Figure 3.12 as function of the scanrate.

Figure 3-13 illustrates that the redox process shown in Figure 3-12 is a diffusion-controlled process. Subsequently, I alsoinvestigated how methylene blue behaves with an 11-mercapto-1-undecanol-modified electrode under a surface-controlled process (whether MB adsorbs on the SAM-modified gold electrode).

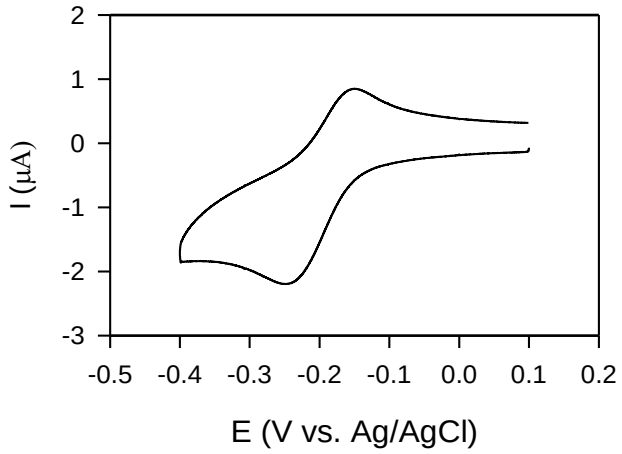

Figure 3-14. CV of surface-adsorbed MB with 11-mercapto-1-undecanol SAM-modified gold electrode in the electrolyte (150 mMLiCl, 10 mMTris,3 mM $MgCl_2$, pH = 7.4); scan rate = 100 mV/s.

Figure 3-14 represents a typical cyclic voltammogram of an 11-mercapto-1-undecanol SAM-modified gold electrode (incubated in 1.0 mM MB for 24 hours) in a MB-free electrolyte.Thedetectable peak current indicates that methylene blue adsorbs on the electrode surface, either directly contacting the gold surface or by incorporationin the11-mercapto-1-undecanol. The apparent surface density of methylene blue is as low as $6x10^{-12}$molecules/cm^2, which is only about 2% of the apparent surface density of MB adsorbed on a bare gold electrode. This may have two reasons: 1) 11-mercapto-1-undecanol molecules are packed densely on the gold surface, resulting in few defects for methylene blue to adsorb; 2) a large amount of methylene blue may be incorporatedin11-mercapto-1-undecanol, but only a fewmolecules near the gold surface areredoxactive.

According to Figure 3-15 we can estimate the apparent electron transfer rate constant of methylene blue adsorbed on the 11-mercapto-1-undecanol-modified gold electrode.Here it is 0.37 s^{-1}, which is 14% of the apparent transfer rate constant of methylene blue directly adsorbed on the gold surface.According to the electron tunneling

mechanism (see Equation 1.1), electron transfer rates decrease exponentially when the electron tunneling distance increases; and the distance between methylene blue and the gold surface in the 11-mercapto-1-undecanol SAM is much larger than that ofmethylene blue contacting the gold directly. Additionally, the dissociation of surface-adsorbed methylene blue fromthe 11-mercapto-1-undecanol-modified electrode is much slower than that from a bare gold electrode. Around 60% MB remained on the surface and a clear well-defined CV can still be observed after one hour incubation in MB-free electrolyte.

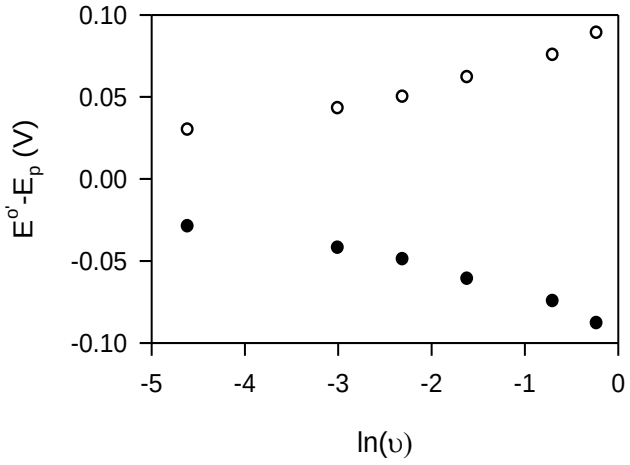

Figure 3-15. Laviron plot of MBadsorbed on11-mercapto-1-undecanol SAM-modified gold electrode in 10 mMTris-HCl, 150 mMLiCl, 3.0 mM $MgCl_2$, 0.1 mM EDTA (pH 7.4) (electrode area = 0.66 cm^2)

In summary, 11-mercapto-1-undecanol SAM hinders the diffusion process of solution-diffused methylene blue and accordingly a much smaller apparentheterogeneous electron transfer rate constant isobtained. The number of MB molecules adsorbed on the surface is much less, and the apparent electron-transfer rate decrease dramatically due to the longer distance between methylene blue and the gold surface.

3.3. **Redox behaviour of methylene blue on11-mercapto-1-undecanoic acidSAM-modified gold electrode**

Besides hydroxyl group-terminated alkanethiols (i.e.,6-mercapto-1-hexanol/$HS(CH)_2OH$) as spacers, researchers have commonly used 11-mercapto-1-undecanoic acid (MUA/$HS(CH_2)_{10}CO_2H$) to immobilizebiomolecules (e.g. cytochrome C).[70,71]Several fundamental aspects regarding how 11-mercapto-1-undecanoic acid interacts with small molecules including methylene blue (MB) have been investigated recently.[67,72] Guided by these previous studies, I used electrochemical methods to study the MB-MUA interactions under the same condition as employed for 11-mercapto-1-undencanol SAM discussed in the previous section.It is possible to estimate the apparent double-layer capacitance of the 11-mercapto-1-undecanoic-acid SAM-modified gold electrode from Figure 3-16. A much smaller double layer capacitance (see Table 3-1.) here may indirectly infer the success of the SAM immobilization.[66]

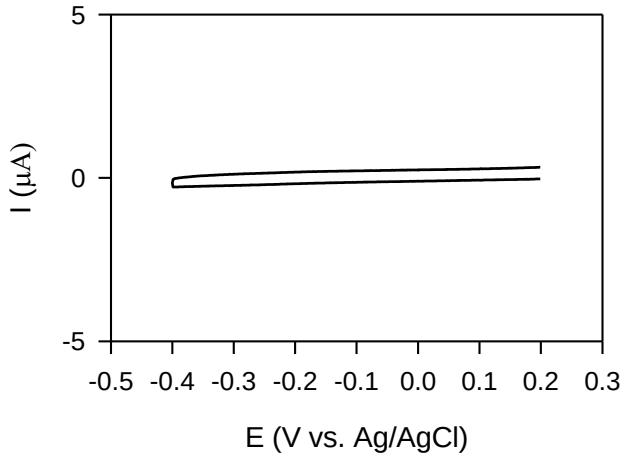

Figure 3-16. CV of 11-mercapto-1-undecanoic acid SAM-modified gold electrode in 150 mMLiCl, 10mMTris, 3mMMgCl$_2$, pH = 7.4); scan rate = 0.1 V/s

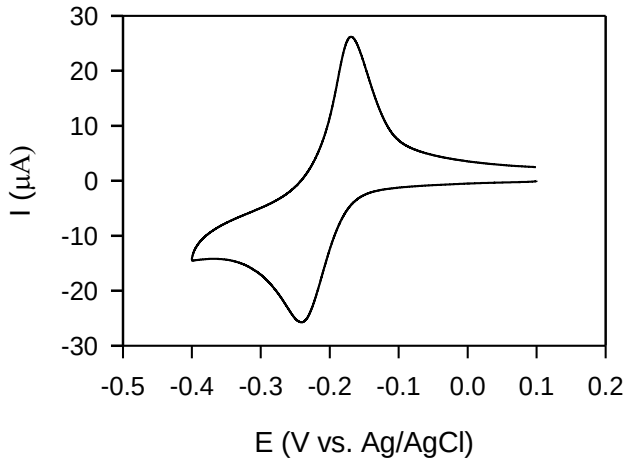

Figure 3-17. 100 µM MB on 11-mercapto-1-undecanoic acid SAM-modified gold electrode in 150 mMLiCl, 10mMTris, 3mMMgCl$_2$, pH = 7.4; scan rate = 0.1V/s

A well-defined redox peak in Figure 3-17 clearly indicates that solution-diffused methylene blue alsopenetrates this SAM and reaches the gold surface. Qualitatively compared with Figure 3-10, the peak separation (E_{pa}–E_{pc}) of the CV in Figure 3-17 is smaller by 193 mV. A quantitativecomparisonshows that the apparentheterogeneous electron transfer rate constant here (4 x 10^{-3} cm/s) is five times larger than that of methylene blue ona 11-mercapto-1-undecanol SAM-modified gold electrode. Because of

the presence of rather lager carboxylate acid groupson MUA monolayer, it typically has less ordered structure than11-mercapto-1-undecanol monolayer, for which methylene blue can diffuse or migrate through the MUA SAM more easily.

The redox properties of MB adsorbed to this SAM were studied by incubatingan MUA-modified gold electrode with methylene blue and then transferring it to anMB free electrolyte.

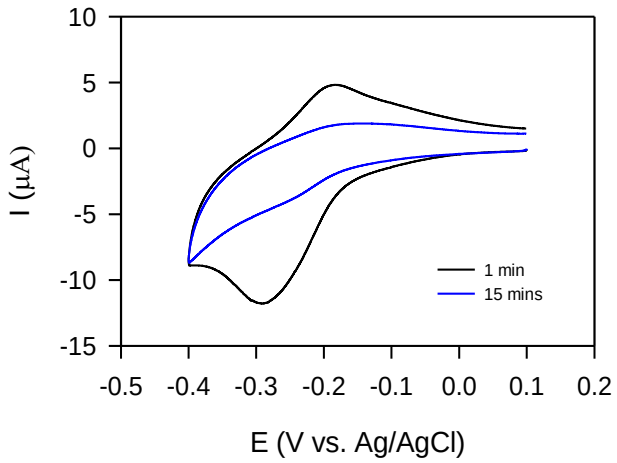

Figure 3-18. CV of surface-adsorbed MB on11-mercapto-1-undecanoic acid-modifiedgold electrode in the electrolyte (150 mMLiCl, 10 mMTris, 3 mM $MgCl_2$, pH = 7; scan rate = 100 mV/s).

According to the CV measuredinthe first minute, the surface density of methylene blue adsorbed on the surfacewas 168 pmol/cm^2,which is about 25 times higherthan that of methylene blue adsorbed on the 11-mercapto-1-undecanol SAM-modified electrode. Such a large number of redox active surface-adsorbed methylene blue indicates that a) there are more “pinholes” on the MUA-modified surface; or b) a large amount of MB accumulated near the surface. The apparenthomogeneous electron transfer rate constant (see Table 3.1) here is also larger than that of methylene blue adsorbed on the 11-mercapto-1-undecanol SAM-modified electrode; it is ofthe same order of magnitude

asthat of methylene blue directly adsorbed on the gold electrode. This supports the conclusion that methylene blue mainly adsorbs directly on the gold surface. Additionally, a relatively faster dissociation process of methylene blue from the electrode to the solution was observed. Only 30% MB remained on the surface after the first 10 minutes and redox peaks disappeared after 15 minutes. As mentioned earlier, an MUASAM has a less ordered and less closely packedstructure than an 11-mercapto-1-undecanol SAM, thus surface-adsorbed methylene blue can diffuse to the solution more easily.Considering earlierresults obtainedbyspectroscopic methods (e.g., Raman spectroscopy, scanning tunneling microscopy (STM), etc.), which show that methylene blue can be trapped at the plane of the carboxylate group on the surface, it is believed that a considerable amount of it can adsorb directly on the gold surface and only few moleculesincorporate with the aliphatic chain.[67,72]

Table 3.1 Summary of data discussed in section 3.

	Electrode Characterization	Solution Control Process	Surface Control Process		
	C_d ($\mu F/cm^2$)	κ (x 10^{-3}cm s^{-1})	k_{app} (x s^{-1})	Γ_{MB} (max. redox active) (pmol/cm^2)	Dissociation Kinetics
Bare-Gold Electrode	~ 24	10 ±12%	2.69 ±8%	267 ±5%	Fast
MCU-Gold Electrode	~ 1.0	0.8 ±20%	0.37 ±5%	6 ±10%	Slow
MUA-Gold Electrode	~ 5.0	4 ±8%	1.77 ±7%	168 ±5%	Fast

3.4. **Summary**

It has been shown that the redox marker methylene blue has quite complex redox properties. Methylene blue and its reduced form can adsorb on gold surfaces; methylene blue can penetrate the SAMs and incorporateintheir alkyl chains. Therefore, when developing any label-free electrochemical biosensors withmethylene blue as solution-diffused redox marker, the experimental conditions to ensure that solution-diffused redox markers do not interferewith the desired electrochemical signals should be carefully chosen.

4. Interaction between methylene blue and a dsDNA-aptamer construct and its sensing application

The research objective of this thesis is to develop a label-free DNA aptamer-based electrochemical biosensor for adenosine, as well asto understandhow methylene blue interacts with thedsDNA-aptamer construct. In the following section, I will discussthe experimental observations and derive conclusions of the thesis work.

4.1. Confirmation of the formation of a dsDNA-aptamer construct

The formation of apt-DNA and comp-DNA constructs were confirmed by non-denaturing gel electrophoresis (Figure 4-1).Either in the presence or in the absence of 1.0 mM adenosine, the lanes of the mixtures of ssDNA strands (1+2, or 1+3) after annealing showed only one band, respectively, with slower mobility than any ssDNA (Figure4-1). This confirms that both apt-DNA (strands 1+2) and comp-DNA (strands 1+3) can form under the specified experimental conditions and that adenosine does not cause de-hybridization of these duplexes. In addition, it was shown that the three ssDNA strands have slightly different gel mobilities. Considering that strands 1 and 2 are guanine-rich, they potentially self-fold to certain tertiary structures that have faster gel mobility than strand 3 (which contains less guanine).[73] Although both strands 1 (in lane 1) and 2 (in lane 2) moved faster than strand 3 (in lane 3), the mixture of strands 1 and 2 (lanes 4 and 5: apt-DNA) moved slightly slower than the mixture of strands 1 and 3

(lanes 6 and 7: comp-DNA) This indicated that the aptamer region affects the gel mobility of the DNA constructs, which further confirmed the formation of a stable DNA conformational switch (apt-DNA).

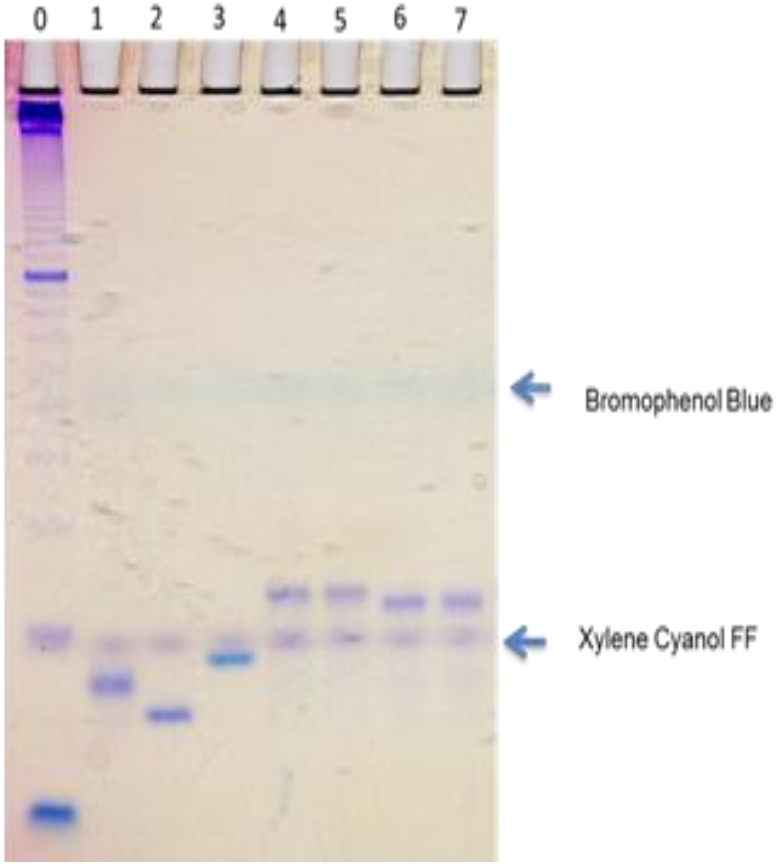

Figure 4-1. ***Gel electrophoresis analysis of the formation of DNA constructs: 14% non-denaturing polyacrylamide gel is run at room temperature at 300 V for 2.5 hours. Lane 0: 10 base-pair ladder marker. Lane 1: strand 1 (thiolated DNA with 22 nucleotides). Lane 2: strand 2 (22 nucleotides forming apt-DNA with strand 1). Lane 3: strand 3 (22 nucleotides forming comp-DNA with strand 1); lane 4: apt-DNA formed by partial hybridization of strands 1 and 2. Lane 5: mixture of strands 1 and 2 incubated overnight with 1.0 mMadenosine.Lane 6:comp-DNAformed by complete hybridization of strands 1 and 3 (22 base pairs).Lane 7: mixture of strands 1 and 3 incubated overnight with 1.0 mM adenosine.***

4.2. Redox behaviour of methylene blue non-covalently bound to the aptamer-DNA construct

4.2.1. Characterization of DNA-modified Au electrode

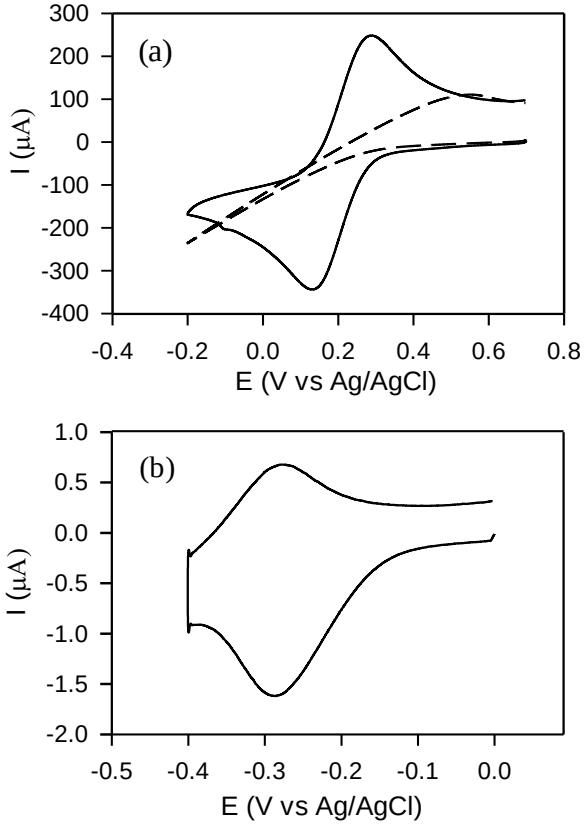

Figure 4-2. ***(a) Cyclic voltammetry of 1.0 mM $K_3Fe(CN)_6$ on bare (solid line) and dsDNA-aptamer construct (apt-DNA)-modified gold electrode (dashed line). The negatively charged DNA strands on the surface repel $Fe(CN)_6^{3-}$ from the electrode and hence no clear redox peaks were observed with the DNA-modified gold electrode. (b) Cyclic voltammetry of 3.5 μM $Ru(NH_3)_6Cl_3$ with the same apt-DNA/MCH-modified gold electrode. $Ru(NH_3)_6^{3+}$ can bind with dsDNA electrostatically, resulting in a pair of symmetric redox peaks around -0.3 V (vs. Ag/AgCl).***

We have used $K_3Fe(CN)_6$ and $[Ru(NH_3)_6]Cl_3$ to confirm that the gold electrodes were modified with DNA monolayer successfully. $K_3Fe(CN)_6$ in solution would generate a

clearly defined redox peak with the bare gold electrode. However, the negatively charged DNA strands on the surface would repel $Fe(CN)_6^{3-}$ from the electrode and hence no clear redox peaks were observed with the DNA-modified gold electrode (as shown in Figure 4-2(a)). We also used $[Ru(NH_3)_6]Cl_3$ to test the DNA-modified surface. As studied previously, positively charged $Ru(NH_3)_6^{3+}$ in solution would bind to the DNA on the surface and generate surface-controlled redox peaks (as shown in Figure 4-2(b)). Thus, combining Figure 4-2(a) and (b), it is confirmed that the gold electrode is modified with a close-packed DNA monolayer.

4.2.2. Confirmation of the redox peak from methylene blue bound to DNA, not from methylene blue incorporatedinalkanethiolate SAM

As mentioned in the previous section, methylene blue can be incorporatedintoalkanethiolate SAMs and generate a surface redox signal. 6-Mercapto-1-hexanol (MCH) is used as spacer in our DNA-modified gold electrode; hence it is necessary for us to identify any possible signal resulting from methylene blue incorporated in MCH. A gold electrode was first modified with 6-mercapto-1-hexanol (MCH)and immersed in 10 M methylene blue in deionized waterfor 15 hours. It was then testedin a MB-free electrolyte. A relatively low concentration of methylene blue is applied here, because low concentrations of methylene blue will be used in future experiments to detect adenosine using the specially designed dsDNA-aptamer construct. Figure 4-3shows the CV of the MB-treated electrode (modified with MCH SAM) in a MB-free electrolyte. It is clear that with a low bulk concentration of methylene blue, given a long incubation time, MCH molecules on the surface barely “trap” any solution-diffused methylene blue.

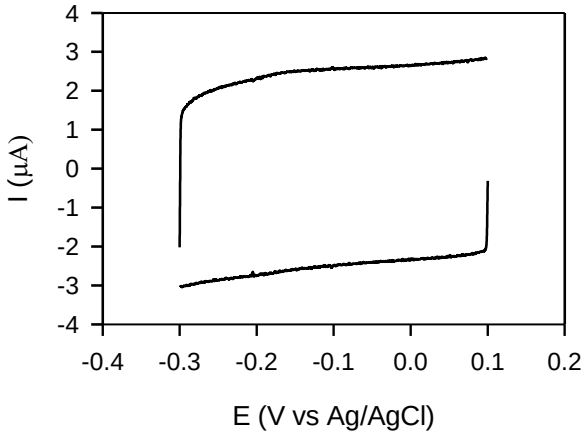

Figure 4-3. Cyclic voltammetry of MCH-modified gold electrode after 15-hour 10 μM MB incubation treatment (electrolyte:10 mMTris-HCl, 150 mMLiCl, 3 mM $MgCl_2$, 0.1 mM EDTA (pH 8.2), electrode area =0.66 cm^2; scan rate =1 V/s).

4.2.3. Cyclic voltammogram of methylene blue non-covalently bound to DNA

Figure 4-3(a) shows the CV curves of 5.0 μM methylene blue on an apt-DNA-modified gold electrode. When the electrode potential was scanned towards negative, MB was reduced to LB (leucomethylene blue) via a two-electron process and protonation. E_{pa} and E_{pc} were observed near -0.26 V and -0.29 V (vs. Ag/AgCl). More importantly, the linear relationship between the scan rate and the cathodic peak current (as shown in Figure 4-3(b).) indicates that MB is bound to the DNA-modified surface. Comparison of the cathodic and anodic peaks reveals that the two peaks are not symmetric, as previously observed by others.[74,75] Their significant separation may be due to the fact that the reduced form, LB, has a different molecular structure, and it is no longer positively charged; the interaction between LB and DNA is not the same as that between MB and DNA.

In another experiment, we investigated the time dependence of the CV response upon adding MB. Figure 4-4 shows that the peak current increased sharply in the first 5

minutes, then gradually reached a plateau (within 30 minutes). Hence, a 30-minute incubation period is required for quantitative analysis such as the adenosine binding study described in the following sections. Upon reaching equilibrium (e.g., after 30 min incubation) we carried out ten consecutive CV scans (without pause) and noticed that the MB peak current decreased dramatically after the first scan and then remained stable. Subsequently, the peak current recovered in a new scan after only 15 seconds. A review of the binding mode between MB and DNA reveals that positively charged MB can associate with DNA via electrostatic interaction with the negatively charged phosphate backbone.[76, 77]On the other hand, the reduced form (LB) is neutral; thus after the first CV scan, neutral LB may dissociatefrom the DNA resulting in a decreased peak current. Non-electrostatically bound MB (namely, intercalated bound MB and guanine stacked MB) would remain on the DNA after several scans and generate a stable signal all the time. After the 15-second period of silence, MB in solution binds again electrostatically to the DNA and the peak current recovers.

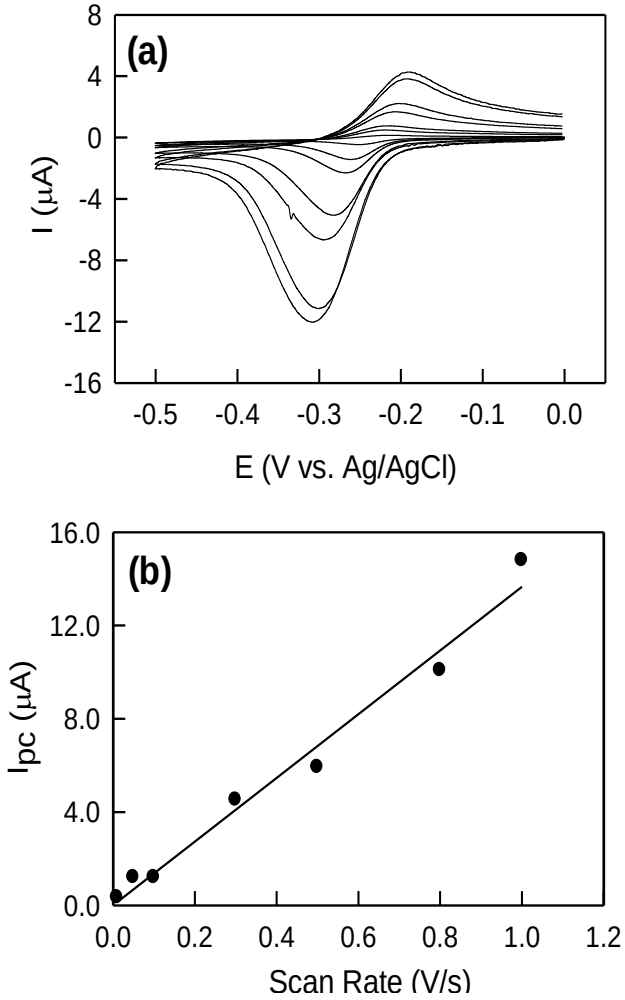

Figure 4-3. ***(a) Cyclic voltammetry of 5.0 µM methylene blue in 10 mMTris-HCl, 150 mMLiCl, 3 mM $MgCl_2$, 0.1 mM EDTA (pH 8.2) at an apt-DNA-modified gold electrode (area = 0.66 cm^2; scan rate = 10, 50, 100, 300, 500, 800, 1000 mV/s). (b) Plot of I_{pc} vs scan rate.***

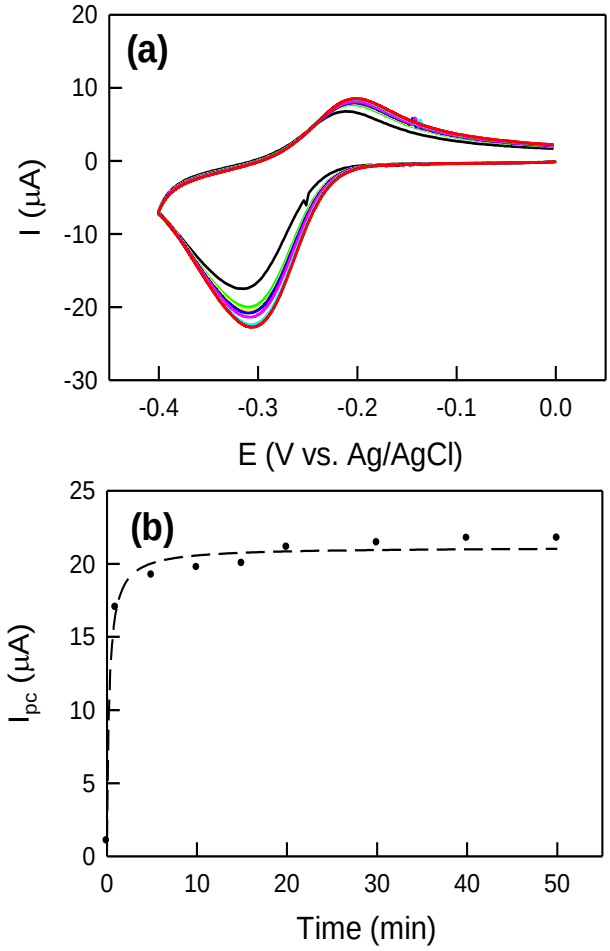

Figure 4-4. ***(a) Cyclic voltammetry of 5.0 μM methylene blue in 10 mMTris-HCl, 150 mMLiCl, 3 mM $MgCl_2$, 0.1 mM EDTA (pH 8.2) at an apt-DNA-modified gold electrode (area = 0.66 cm^2; scan rate = 1 V/s). The colored curve represents the CV of MB after different incubation times (from black to red, the MB incubation times increased from 5 to 50 min). (b) Plot of I_{pc} vs. incubation time of MB.***

We also calculated the electron transfer rate constants of the DNA-surface-bound MB. As shown in Figure 4-3(a), ΔE_p increased as a function of the scan rate, a phenomenon previously observed by Kelley et al.[17] They reported a cathodic potential of -0.25 V (vs. SCE) for MB intercalating with dsDNA and an increasing ΔE_pat faster scan rates. One possible reason is that the terminal aliphatic chain slows the electron transfer rate of the

MB intercalating apt-DNA system.[78]

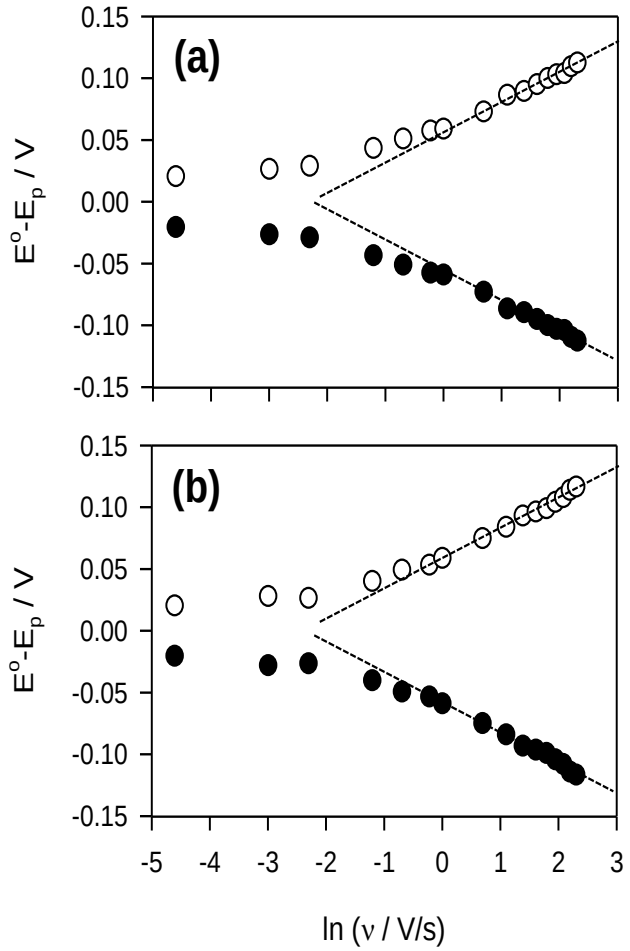

Figure 4-5. Laviron plots of 5.0 µM MB at apt-DNA-modified gold electrode in 10 mMTris-HCl, 150 mMLiCl, 3.0 mM $MgCl_2$, 0.1 mM EDTA (pH 8.2) (electrode area = 0.66 cm^2) before (a) and after (b) incubation with 0.5 mM adenosine. The dashed lines are linear fits to the data at high scan rate (> 10 V/s). Thus determined apparent electron transfer rate constants are 3.8±0.4 s^{-1} and 4.6±0.3 s^{-1} for the case before and after adenosine binding, respectively.

Based on the Laviron theory,[52] the observed electron transfer rate constant k and the transfer coefficient α were found to be 3.8 ± 0.4 s^{-1} and 0.55 ± 0.02, respectively, i.e., much smaller than k = 1500 s^{-1} for MB adsorbed to mercury,[79] an indication that MB is located farther away from the electrode surface.

4.3. **Multiplex interaction between methylene blue and the aptamer-DNA construct**

The anti-adenosine DNA aptamer was originally selected by Huizenga and Szostak;[31] its structure has been well characterized by Lin and Petal.[32] It is interesting to examine whether the interaction modes between MB and apt-DNA change upon binding adenosine. As shown in Figure 4-6(a), the peak current of MB decreased after introducing 1 mM adenosine to the apt-DNA-modified electrode, and recovered after removal of the adenosine. In contrast, there is no signal change after adding adenosine to the comp-modified electrode (Figure 4-6(b)). In their high-resolution NMR studies, Lin and Patel have confirmed that one DNA aptamer accommodates two AMP molecules by self-adaptive folding to a tight structure with facilitated base stacking.[32] Upon AMP binding, the 'unstructured asymmetric internal loop' of the aptamer domain folds into two parallel triple-base platforms, widening the minor groove. Patel et al. summarized later that aptamers would usually show an induced-fit folding behavior upon target binding.[32,33]Therefore, initially we had expected that the adenosine binding-induced formation of DNA triple-base platforms would allow more MB to intercalate in the DNA construct. Accordingly an increased peak current of MB should be observed upon incubation with adenosine.

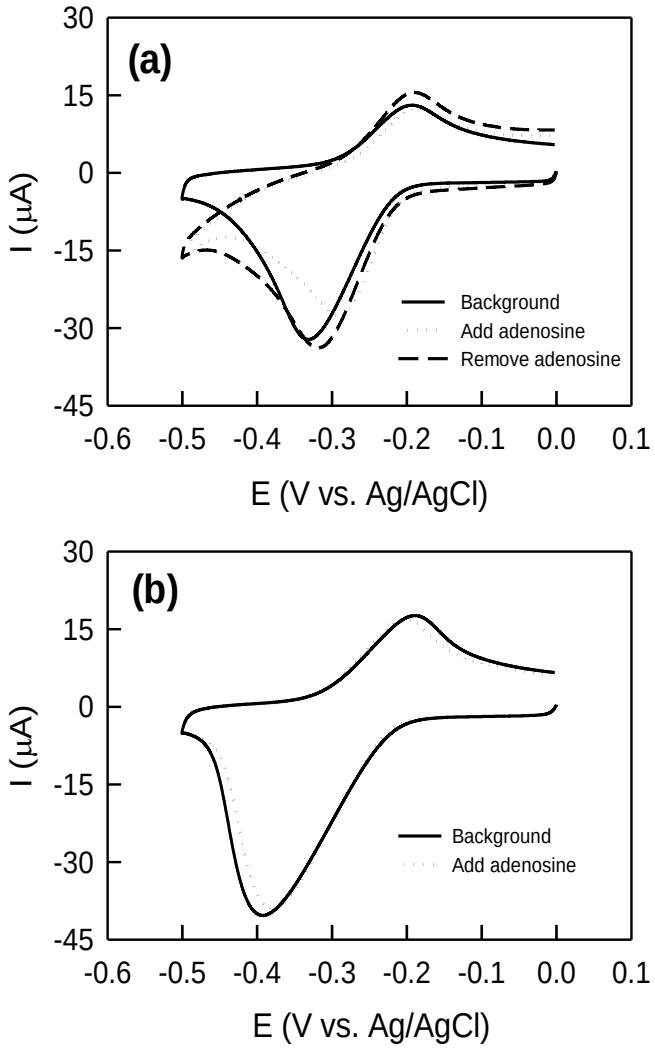

Figure 4-6. ***Electrochemical response of apt-DNA and comp-DNA upon incubation with adenosine. (a) CV curves of 10 µM MB at an apt-DNA-modified gold electrode in 10 mMTris-HCl, 150 mMLiCl, 3 mM $MgCl_2$, 0.1 mM EDTA (pH 8.2) (electrode area = 0.66 cm^2; scan rate = 1 V/s). The solid line is the signal before adding adenosine, the signal after adding adenosine is shown as dotted line. The dashed line represents the signal after removing adenosine. (b) CV curves of 10 µM MB at a comp-DNA-modified gold electrode in 10 mMTris-HCl, 150 mMLiCl, 3 mM $MgCl_2$, 0.1 mM EDTA (pH 8.2) (area = 0.66 cm^2; scan rate = 1V/s). The solid line represents the signal before adding adenosine, the signal after adding adenosine is shown as a dashed line.***

Considering the slight increase of the apparent electron transfer rate constant (4.6 ±0.3 s^{-1}) upon adding adenosine, we believe that this surprising decrease in the peak current of MB is due to a conformational change of the aptamer domain. The most likely reason is that originally MB was stacked with a single guanine base in the aptamer domain;[47,48]upon adenosine-induced conformational change this MB was eliminated and released into solution.

In order to estimate the number of MB molecules bound to either apt-DNA or comp-DNA, we must determine the ratio of DNA duplex and MB surface densities. The surface density of the DNA-bound MB (Γ_{MB}) and DNA is obtained by the method described in Section 2.2.5.1..A typical CV of $Ru(NH_3)_6^{3+}$ on an apt-DNA-modified gold electrode is shown in Figure4-7. The DNA surface density clearly did not change on addition of adenosine (the difference is less than 10%). This further confirms that the apt-DNA constructs are stable on the gold electrode when adenosine binds, i.e., no dehybridization or desorption takes place. We originally expected that a maximum of 7 MB molecules would bind to each comp-DNA due to its rich GC base pair content.[80]The result is rather surprising; only one MB (0.98 ± 0.05) molecule was bound to each comp-DNA, and the presence of adenosine in solution had no influence on this value. Kelley et al. obtained similar results,[74] and proposed that a tightly packed comp-DNA film on the surface restricts the access of solution-diffused MB to the potential binding sites. After the first MB binding, there is little chance for another MB to bind. Thus we believe that only one MB molecule (average 0.98±0.05) intercalates with GC pairs at the solution end of the comp-DNA. In comparison, we found that at least two MB molecules were bound to apt-DNA (2.3 ± 0.2). Considering the structural differences between comp-DNA and apt-DNA, the extra MB is probably binding to the guanine-rich aptamer domain. By immobilizing a series of synthetic ssDNA containing different numbers of guanine bases

on a carbon paste electrode and making electrochemical measurements in MB solution, Yang et al. have shown that guanine bases in ssDNA have a specific affinity for MB. In particular, they found that the peak area of MB reduction increases with the number of guanine bases present in the ssDNA.[47] Moreover, a molecular dynamics simulation led Enescu et al. to propose a "stacking" conformation for the structure of guanine-MB complexes in water. The above findings support the likelihood that in apt-DNA the extra MB binds to the aptamer domain, as the guanine bases in this unstructured section behave like guanine bases in ssDNA.[48]

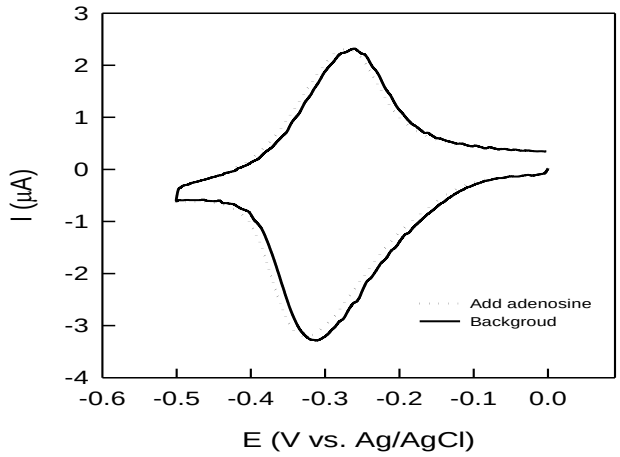

Figure 4-7. CV plots of 3.5 μM $Ru(NH_3)_6^{3+}$ in 10 mMTris (pH = 8.2) at an apt-DNA-modified gold electrode (electrode area = 0.66 cm^2; scan rate = 100 mV/s) before and after binding adenosine. The surface density of apt-DNA can be determined by integration of the reduction peak.

It should be noted that the above comparison holds for DNA films with the relatively low DNA surface density of 2×10^{11} to 7×10^{11} molecule/cm^2. At higher DNA surface densities substantially smaller numbers of MB molecules were measured for both apt-DNA and comp-DNA (Figure 4-8). More importantly, it is evident that within the same DNA surface density range, the number of MB bound to apt-DNA is always around twice that on comp-DNA, indicating that even at higher surface densities of apt-DNA, additional MB can stack in the aptamer domain. According to the hypothesis of Kelley et

al.,[74] only one MB molecule should intercalate between the terminal GC pairs of both apt-DNA and comp-DNA. In fact,as shown in Figure 4-8,on average 1.0 MB and 0.5 MB are bound to apt-DNA and comp-DNA, respectively, when the surface density becomes high (~ 5×10^{12} molecule/cm^2). Here we have not considered the heterogeneity of the DNA films,[81] which also influences the possibility of MB intercalation in the DNA double helices.

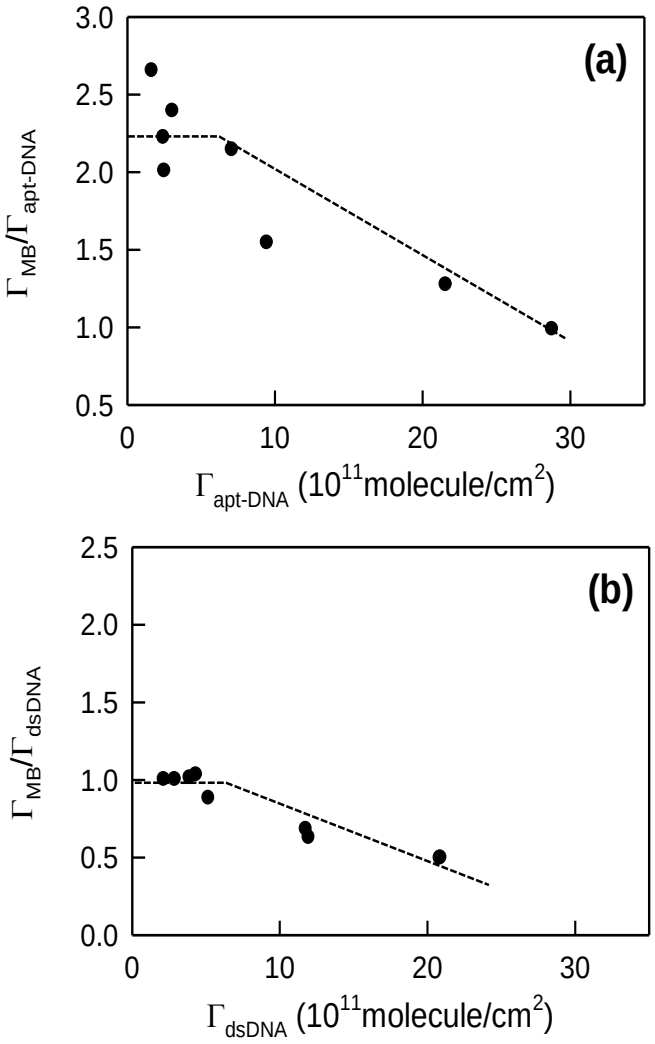

Figure 4-8. ***The number of MB molecules bound to (a) apt-DNA and (b) comp-DNA as function ofthe apparent surface density of DNA constructs immobilized on a gold electrode.Each data point was calculated from an on-chip (electrode) CV experiment with 1.0 µM MB without adenosine in binding buffer (electrode area = 0.66 cm^2; scan rate = 100 mV/s). The dashed lines are to guide the eyes only.***

All the above results can be interpreted with the schematic view of the differently boundMB molecules on apt-DNA (shown in Figure 4-8.) It is possible that one MB intercalates between the GC pairs located near the solution-electrode interface; one extra MB can reversibly stack with the single guanine base in the aptamer domain of the

DNA conformational switch. By introducing or removing the adenosine, this MB can be eliminated into solution or re-bind with the aptamer domain.

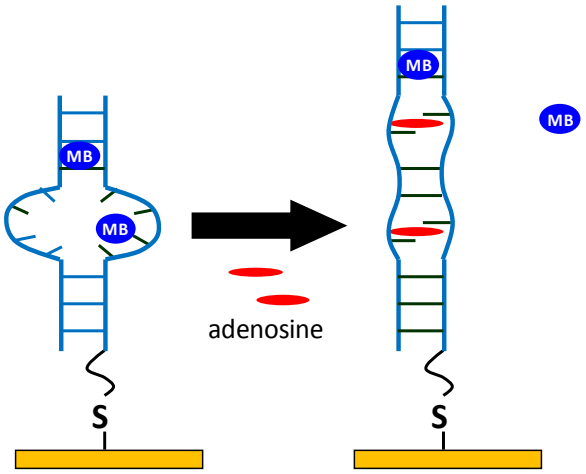

Figure 4-9. ***Schematic comparison of the binding modes of MB to the dsDNA-aptamer construct (apt-DNA) before and after adenosine binding. An MB molecule intercalates in the upper stem of apt-DNA which is not influenced by the adenosine binding. The extra MB on a single guanine in the aptamer domain of apt-DNA is eliminated upon adding adenosine, resulting in the formation of a structurally more compact aptamer-ligand complex.***

4.4. Sensing aspects and the adenosine/apt-DNA binding isotherm

Compared with gel electrophoresis assay-based biochemical studies,[34] our electrochemical approachis more suitable for investigating the reversibility and selectivity of this DNA conformational switch for binding adenosine. Figure 4-10 shows that addition of AMP and adenosine resulted in a positive response (decreased peak current) while GMP and UMPcausedrelatively less significant (but discernible) changes.It has been reported that the same DNA aptamer binds ATP, AMP and adenosine with similar binding affinities.[30]Although the relative binding affinity of adenosine vs. AMP to the DNA aptamer was not evaluated previously, the lower signal obtained for AMP may be due to the interaction of the phosphate group with the negatively charged DNA backbone. The reason for the “negative” signal observed when adding UMP and GMP is not known at this stage, especially the aptamer sequence was originally selected for binding ATP/adenosine.[30,32]An NMR study by Noeske et al.[82] showed that the aptamers of both guanine and adenosine form intramolecular triplets; the addition of large amounts of GMP may induce the formation of inter-chain constructs, which in turn increase the number of MB molecules intercalated into the film.

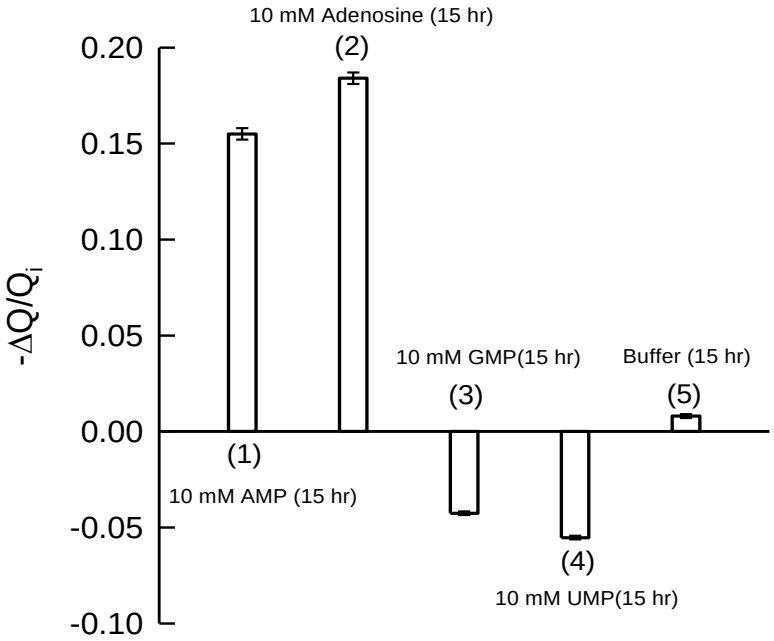

Figure4-10. Relative electrochemical signal change ($\Delta Q/Q_i$) for background, positive and negative controls by adding 1.0 μM MB at an apt-DNA-modified gold electrode: The relative signal decrease normalized over the surface density is plotted: (1) 15-hour incubation with 10 mM AMP; (2) 15-hour incubation with 10 mM adenosine; (3) 15-hour incubation with 10 mM GMP; (4) 15-hour incubation with 10 mM UMP; (5) 15-hour incubation with binding buffer.

Figure 4-11(a) shows that the response signal ($-\Delta Q/Q_i$) initially increaseswith increasing concentration of adenosine in the electrolyte, and reachesa plateau above 300 μM. Based on the Langmuir model,[51] we further evaluated the first-order dissociation constant of the adenosine/apt-DNA complex on the electrode surface. The classical Langmuir model assumes that every binding site is equivalent and that the ability of a molecule to bind is independent of the occupation of nearby sites. A linearized form of the Langmuir isotherm which correlates the adenosine concentration (*C*) in solution, the

electrochemical signal ($\Delta Q/Q_i$), the saturated signal change $(\Delta Q/Q_i)_{sat}$ and the dissociation constant K_d is given by Equation 4-1:

$$\frac{C}{(\Delta Q/Q_i)} = \frac{C}{(\Delta Q/Q_i)_{sat}} + \frac{K_d}{(\Delta Q/Q_i)_{sat}} \quad \text{(Equation 4-1)}$$

In Figure 4-11(b) the value of $\frac{C(\Delta Q/Q_i)_{sat}}{(\Delta Q/Q_i)}$ is plotted as a function of the adenosine concentration (*C)*. From the fitted intercept, we can determine the dissociation constant K_d of the adenosine/apt-DNA complex. The value obtained here (88±10 μM) shows a moderate improvement from that of the strand-displacement design (127 μM),[83] and that from gel electrophoresis experiments (135 μM).[34]

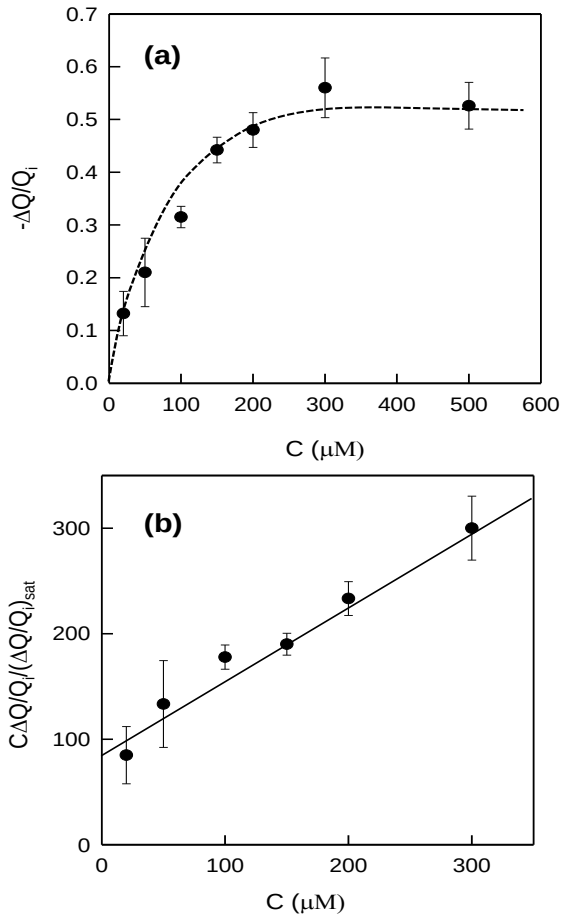

Figure 4-11. (a) Plot of relative electrochemical signal change as a function of adenosine concentration. Error bars show the variance of data points obtained in three independent CV measurements. The dashed line is to guide the eyes only. (b) A linearized isotherm of adenosine binding to the immobilized dsDNA-aptamer construct.

With MB as model system, we are able to illustratethe “multiplex” modes of binding between “intercalative” small molecules and specially designed dsDNA-aptamer constructs. This will eventually augment the design and construction of the next generation of DNA-based sensing and switching devices with good sensitivity and reproducibility. Thereported dissociation constant of adenosine/apt-DNA indicates a moderate binding affinity of the designed dsDNA-aptamer construct for the target ligand on the electrode surface. Several novel strategies to enhance the electrochemical signal

in aptamer-based biosensors for adenosine/ATP have been proposed recently,[84-89] e.g., the use of functionalized gold nanoparticles. In conjunction with these novel approaches for signal enhancement, it is entirely possible to develop an ultrasensive adenosine (or other small molecular ligand) sensor based on the design principle of functional dsDNA-aptamer constructs.

4.5. **Summary**

We have demonstrated that solution-diffused MB can interact with a surface-immobilized dsDNA-aptamer construct in at least two different modes, namely intercalation and single-base stacking. Based on the surface densities of dsDNA and MB determined by cyclic voltammetry we have shown that one MB molecule can intercalate in a 22-mer dsDNA. Depending upon the surface density of the dsDNA-aptamer construct, at least one extra MB can stack in the aptamer domain, and an adenosine binding-triggered conformational change causes the elimination of this extra MB. The dissociation constant of the adenosine/apt-DNA complex was determined from the binding isotherm, which is a moderate improvement over gel electrophoresis assays and the strand-displacement design.

5. Summary and concluding remarks

In this thesis, I have gradually improvedmy understanding of the challenges in the design of a label-free electrochemical biosensor through a comprehensive study of the electrochemical properties of MB. In the first phase, I examined the redox behaviour of the solution-diffusedredox marker methylene blue at a bare gold electrode. It was confirmed that methylene blue undergoes a one-proton coupled two-electron redox process in thephysiological pH range and both methylene blue and leocumethylene blue can adsorb on gold surface.

Next, I have studied how methylene blue interacts with alkanethiolateSAMs on gold. Combined with theliterature results, it was concluded that methylene blue can penetrate the SAMs of alkanethiols and incorporateinthe alkane chains. SAMs formed by carboxyl-terminated alkanethiols can leave more “channels” for methylene blue to migrate or diffuse. Thus a higher electron transfer rate constant is found for 11-mercapto-1-undecanoic acid SAM-modified gold electrodethan for an electrode modified with an11-mercaptol-1-undecanol SAM.

After investigating the redox behaviour of methylene blue on bare and SAM-modified gold electrodes, a label-free electrochemical biosensor using solution-diffused methylene blue as redox marker was designed and tested. Besides testing its sensitivity, the signallingmechanismwas examined; it was found that one MB molecule can intercalate in a 22-mer dsDNA; depending upon the surface density of the dsDNA-aptamer construct, at least one extra MB can stack in the aptamer domain, and an

adenosine binding-triggered conformational change causes the elimination of this extra MB.

The main spirit of this thesis is that fundamental research on the surface chemistry is critical to the development of biosensors. Although such fundamental research may not be a rapid means to obtain a higher sensitivity of a biosensor, it can guide us to find areliablesignaltransduction path.

References

1. Blackburn, G.M.; Gait, M.J. Introduction and overview. In *Nucleic acids in chemistry and biology*; Blackburn, G.M.; Gait, M.J., Eds.; Oxford University Press: New York, 1990; p. 3-4.

2. Blackburn, G.M. DNA and RNA structure. In *Nucleic acids in chemistry and biology*; Blackburn, G.M.; Gait, M.J., Eds.; Oxford University Press: New York, 1990; p. 17-20.

3. Manning, G.S. *Ann. Rev. Phys. Chem*., **1972**, 23, 117-140

4. Manning, G.S. Acc. Chem. Res., **1979**, 12, 443-449

5. Wilson, W.D. Reversible interactions of nucleic acids with small molecules. In *Nucleic acids in chemistry and biology*; Blackburn, G.M.; Gait, M.J., Eds.; Oxford University Press: New York, 1990; p. 295.

6. L.S. Lerman, *J. Mol. Biol.*, **1961**, 3, 18-30

7. Wilson, W.D.; Tanious, F.A.; Barton, H.J.; Strekowski, L.; Boykin, D.W.; Jones, R.L. *J. Am. Chem. Soc.*, **1989**, 111, 5008-5010

8. Eley, D. D.; Spivey, D. I. *Trans. Faraday Soc*., **1962**,58, 411-414

9. Debije, M.G; Milano, M.T.; Bernhard, W.A. *Angwe. Chem. Int. Ed.*, **1998**, 38, 2752-2756

10. Kasumov, A.Y.;Kociak, M.;Gueron, S. *Science*, **2001**, 291, 280-282

11. Park, S.J.;Taton, T.A.; Mirkin, C.A.*Science*, **2002**, 295, 1503-1506

12. Fink, H.W.;Schonenberger, C.*Nature*, **1999**, 398, 407-410

13. Giese, B. Current Opinion in Chemical Biology,**2002**, 6, 612-618

14. Lewis, F.D.; Letsinger, R.L.;Wasielewski, M. R. *Acc. Chem. Res.*, **2001**,34,159-170

15. Prigogine, I.; Rice, S.A. *Adv. Chem. Phys*., **1999**, 106, 35-202

16. Barton, J.K.; Kumar, C.V.;Turro, N.J. *J. Am. Chem. Soc.,***1997**, 119,9861-9870

17. Kelley, S.O.; Holmlin,R.E.; Stemp, E.D.A.; Barton, J.K.*J. Am. Chem. Soc.*, **1993**, 262, 1025-1029

18. Hall. D.B.; Holmlin, R.E.; Barton, J.K. *Nature*, **1996**,382, 731-735

19. Chung, M.H.; Kiyosawa, H.; Nishimura, S. *Biochem. Biophys. Res. Commun*., **1992**, 188, 1-7

20. Wackerbarth, H.; Zhang, J.; Grubb, M.; Hansen, A.G.; Ooi, B.L.; Christensen, H.E.M.; Ulstrup, J. Self-Assembly of Biomolecules on Electrode Surfaces; Oligonucleotides, Amino Acids, and Proteins toward the Single-Molecule Level. In *Electrochemistry of nucleic acids and proteins – towards electrochemical sensors for genomics and proteomics*; Palecek, E.; Scheller, F.; Wang, J. Eds.; Elsevier B.V.: Amsterdam, 2005; 1stedn., Chapter 15, p. 485-511.

21. Love, J.C.; Estroff, L.A.; Kriebel, J.K.; Nuzzo, R.G.; Whitesides, G.M. *Chem. Rev*., **2005**, 105, 1103-1170

22. Steel, A.B.; Levicky, R.L.; Levicky; Herne, T.M.; Tarlov, M.J. *Biophys. J.*, **2000**, 79, 975-981

23. Herne, T.M.; Tarlov, M.J. *J. Am. Chem. Soc.*, **1997**, 119, 8916-8920

24. Petrovykh, D.Y.; Kimura-Suda, H.; Whitman, L.J.; Tarlov, M.J. *J. Am. Chem. Soc*., **2003**, 125, 5219-5226

25. Levicky, R.; Herne, T.M.; Tarlov, M.J.; Satija, S.K.; *J. Am. Chem. Soc*., **1998**, 120, 9787-9792

26. Tuerk, C.; Gold, L. *Science*, **1990**, 249, 505-510

27. Ellington, A.D.; Szostak, J.W. *Nature*, **1990**, 346, 818-822

28. Ellington, A.D.; Szostak, J.W. *Nature*, **1992**, 355, 850-852

29. Wilson, D.S.;Szostak, J.W. *Ann. Rev. Biochem*., **1999**, 68, 611-647

30. Sassanfar, M.; Szostak, J.W. *Nature*, **1993**, 364, 550-553

31. Huizenga, D.E.; Szostak, J.W. *Biochemistry*, **1995**, 34, 656-665

32. Lin, H.C.; Petal, J.D*; Chemistry & Biology*,**1997**, 4,817-832

33. Herman, T.; Patel, D.J. *Science*, **2000**, 287, 820-825

34. Fahlman, R.P.; Sen, D. *J. Am. Chem. Soc*., **2002**, 124, 4610-4616

35. Xiao, Y.; Lubin, A.A.; Heeger, A.J.; Plaxco, K.W. *Angew. Chem. Int. Ed.,***2005**, 44, 5456-545

36. Huang, Y.C.; Ge, B.; Sen, D.; Yu, H.Z. *J. Am. Chem. Soc*. **2008**, 130, 8023-8029

37. Cheng, A.K.H.; Ge, B.; Yu, H.Z. *Anal. Chem.,***2007**, 79, 5158-5164

38. Bang, G.S.; Cho, S.; Kim, B.G. *Biosensors and Bioelectronics*, **2005**, 21, 863-870

39. Bergmann, K.; O'Konski, C.T. *J. Phys. Chem.,***1963**, 67, 2169

40. Kipling, J.J.; Wilson, R.B. *J. Appl. Chem*., **1960**, 10, 109-113

41. Bridicka, R.; Knobloch, E.Z. *Electrochem*., **1941**, 47, 721-723

42. Tuite, E.; Kelly, *J.M. Biopolymers*, **1982**, 21, 1713-1734

43. Tuite, E.; Norden, B. *J. Am. Chem. Soc*., **1994**, 116, 7548-7556

44. Norden, B.; Tjerneld, F. *Biopolymers*, **1982**, 21, 1713-1734

45. Bardley, D.F.; Stellwagen, N.C.; O'konski, C.T.; Paulson, C.M. *Biopolymers*, **1972**, 11, 645-652

46. Nafisi, S.; Saboury, A.A.; Keramat, N.; Neault, J.F.; Tajmir-Riahi, H.A. *J. Mol. Struct.*, **2007**, 827, 35-43

47. Yang,W.; Ozsoz, M.; Hibbert, B.D.; Gooding, J.*J. Electroanalysis*, **2002**, 18, 1299-1302

48. Gheorghe, V.; Levy, B.; Enescu, M. *J. Phys. Chem. B.,***2000**,104, 1073-1077

49. Yu, H.Z.; Luo, C.Y.; Sankar, CG.;Sen, D. *Anal. Chem*.,**2003**, *75*, 3902-3907

50. Ge,B.; Huang, Y.C.; Sen, D.; Yu, H.Z.*J.Electroanal. Chem.*,**2007**, *602*, 156-162

51. Su, L.; Sankar, C.G.; Sen, D.; Yu, H.-Z. *Anal.Chem*.,**2004**, *76*, 5953-5959.

52. Laviron, E. *J. Electroanal. Chem*.,**1979**, 101, 19-28.

53. Nicholson, R.S. *Anal. Chem*., **1965**, 37, 1351-1355

54. Arvia, A.J.; Hahn, F.; de Tacconi, N.R.; Lezna, R.O. *J. Electroanal. Chem*., **1991**, 306, 259-269

55. Naujok, R.R.; Duevel, R.V.; Corn, R.M. *Langmuir*, **1993**, 9, 1771-1774

56. Zutic, V.; Svetlicic, V.; Clavilier, J. *J. Electroanal. Chem.,* **1996**, 402, 129-135

57. Bard, A.J. Controlled Potential Microelectrode Techniques – Potential Sweep Methods. In *Electrochemical Methods*; Bard, A.J.; Faulkner, L.R. Eds.; John Wiley & Sons, Inc.: Toronto, 1980; 1stedn.,Chapter 6, p. 213-219.

58. Vetter, K.J.; Bardeleben, J. *Z. Elektrochem*., **1967**, 61, 135-137

59. Yu, H.Z.; Wang, Y.Q.; Cheng, J.Z.; Zhao, J.W.; Cai, S.M.; Inokuchi, H.; Fujishima, A.; Liu, Z.F. *Langmuir*, **1996**, 12, 2843-2848

60. Zhan, R.; Song, S.; Liu, Y.; Dong, S. *J. Chem. Soc., Faraday Trans*., **1990**, 86, 3125-3127

61. Wopschall, R.H.; Shain, I. Anal. Chem., **1967**, 39, 1514-1527

62. Wopschall, R.H.; Shain, I*. Anal. Chem*., **1967**, 39, 1527-1534

63. Yang, Y.C.; Chang, T.Y.; Lee, Y.L. *J. Phys. Chem. C.,***2007**, 111, 4014-4020

64. Groat, K.A.; Creager, S.E. *Langmuir*, **1993**, 9, 3668-3675

65. Finklea, H.O. *J. Electroanal. Chem*. **1996**, 19, 109-112

66. Sagara, T.; Kawamura, H.; Nakashima, N. *Langmuir*, **1996**, 12, 4253-4259

67. Tognalli, N.G.; Fainstein, A. *J. Phys, Chem. B*., **2006**, 110, 354-360

68. Grumelli, D.; Mendez De Leo, L.P.; Bonazzola, C.; Zamlynny, V.; Calvo, E.J.; Salvarezza, R.C. *Langmuir*, **2010**, 26, 8226

69. Benitez, G.; Vericat, C.; Tanco, S.; Lenicov, F.R.; Castez, M.F.; Vela, M.E.; Salvarezza, R.C. *Langmuir*, **2004**, 20, 5030-5037

70. Hobara, D.; Imabayashi, S.; Kakiuchi, T. *Nano Lett*.,**2002**, 2, 1021-1025

71. Vela, M. E.;Martin, H.; Herna´ndezCreus, A.; Andreasen, G.; Salvarezza, R. C. *Langmuir*,**2001**, 17, 6647-6654

72. Vericat, C.; Lenicov, F.R.; Tanco, S.; Andreasen, G.; Vela, M.E.; Salvarezza, R.C.; *J. Phys. Chem. B.***2002**, 106, 9114-9121

73. Simonsson,T. *Biol.Chem***. 2001**, 382, 621-628

74. Kelley, S.O.; Barton, J.K.; Jackson, N.M.; Hill, M.G. *Bioconjugate Chem*.,**1997**, 8, 31-37

75. Boon, E.M.; Jackson, N.M.; Wightman, M.D.; Kelley, S.O.; Hill, M.G.; Barton, J.K. *J. Phys. Chem. B*., **2003**, 107, 11805-11812

76. Tani, A.; Thomson, A.J.; Butt, J.N. *Analyst,* **2001**, 126, 1756-1759.

77. Castano-Alvarez, M.; Fernandez-la-Villa, A.; Fernandez-Abedul, M.T.; Costa-Garcia, A. *Electrophoresis*,**2007**, 28, 4679-4689.

78. Slinker, J.D.;Muren, N.B.; Renfrew, S.E.; Barton, J.K. *Nat. Chem.,***2011**, 3, 228-233

79. Zutic, V.; Svetlicic, V.; Lovric, M.; Ruzic, I.; Chevalet, J. *J. Electroanal. Chem.*, **1984**, 177, 253-268

80. Crothers, D.M. *Biopolmers*,**1968**, 6, 575-584

81. Murphy, J.N.; Chang, A.K.; Yu, H.Z.; Bizzotto, D. *J. Am. Chem. Soc*., **2009**, 4042-4050

82. Noeske, J.; Richter, C.; Grundl, M.A.; Nasiri, H.R.; Schwalbe, H.; Wohnert, J.*Proc. Natl. Acad. Sci., USA,***2005**,102, 1372-1377.

83. Chakraborty, B.; Jiang, Z.; Li, Y.; Yu, H.-Z. *J. Electroanal.Chem*., **2009**, 635, 75-82.

84. Monstserrat, J.M.; Ramirez, S.A.; Ponce, B.; Ceretti, H. *Electroanlysis*,**2009**, *22*, 147-150

85. Zayats, M.; Huang, Y.; Gill, R.; Ma, C.A.; Willner, I. *J. Am. Chem. Soc.*,**2006**, 128, 13666-13667

86. Zhang, S.; Xia, J.; Li, X. *Anal. Chem.*,**2008**, 80, 8382-8388

87. Liu, Z.; Yuan, R.; Chai, Y.; Zhuo, Y.; Hong, C.; Yang, X.; Su, H.; Qian, X. *Electrochim. Acta*,**2009**, 54, 6207-6211

88. Feng, K.; Sun, C.; Kang, Y.; Chen, J.; Jiang, J.; Shen, G.; Yu, R.Q. *Electrochem.Comm.,* **2008***,* 10*, 531-535.*

89. Zuo, X.; Song, S.; Zhang, J.; Pan, D.; Wang, L.; Fan, C. *J. Am. Chem. Soc.,* **2007**, 129, 1042-1043

90. Zhu, L.; Zhao, R.; Wang, K.; Xiang, H.; Shang, Z.; Sun, W. *Sensors,***2008**, 8, 5649 -5660